

IMPROVED INFERENCE ON RISK MEASURES FOR UNIVARIATE EXTREMES

BY LÉO R. BELZILE¹ AND ANTHONY C. DAVISON²

¹*Département de sciences de la décision, HEC Montréal,
3000, chemin de la Côte-Sainte-Catherine, Montréal (QC), Canada H3T 2A7*

²*Institute of Mathematics, EPFL, Station 8, 1015 Lausanne, Switzerland*

We discuss the use of likelihood asymptotics for inference on risk measures in univariate extreme value problems, focusing on estimation of high quantiles and similar summaries of risk for uncertainty quantification. We study whether higher-order approximation based on the tangent exponential model can provide improved inferences, and conclude that inference based on maxima is generally robust to mild model misspecification and that profile likelihood-based confidence intervals will often be adequate, whereas inferences based on threshold exceedances can be badly biased but may be improved by higher-order methods, at least for moderate sample sizes. We use the methods to shed light on catastrophic rainfall in Venezuela, flooding in Venice, and the lifetimes of Italian semi-supercentenarians.

1. Introduction. Estimating worst-case scenarios is important for risk management and policy making, but the hypothetical events that keep decision-makers awake at night can lie far outside the available data. Large-sample likelihood approximations are routinely used for inference based on extreme observations, but the numbers of rare events can be small, which raises the question of the adequacy of standard asymptotic approximations. This concern has led to the development of improved approximations that are used in other domains (e.g., Brazzale et al., 2007), but which have had limited impact in extreme-value statistics.

A key parameter in modelling univariate extremes, commonly known as the extremal index or shape parameter and denoted by ξ , determines how the tail probability declines at extreme levels. A negative value of ξ yields a distribution with bounded support, whereas zero or positive values of ξ yield unbounded extremes, with the distribution tail of form $x^{-1/\xi}$ for large x , so larger values of ξ correspond to increasingly heavy tails. Many authors have studied likelihood inference for ξ and other parameters of extreme value distributions, including Pires et al. (2018), who focused on the shape parameter of the generalized Pareto distribution, and Giles et al. (2016) and Roodman (2018), who considered bias-corrected estimates of extreme-value parameters. Although inferences on ξ give qualitative insights into rare event probabilities, the focus in applications is typically on measures of risk, such as exceedance probabilities for particular values of x , quantiles or related summaries of the tail distribution. Accurate small-sample inference for these risk measures is the topic of this paper.

We outline the use of variants of the profile likelihood and the tangent exponential model approximation for inference and use simulation to assess whether higher-order asymptotic approximations provide improved inferences. We conclude that the coverage properties of

Keywords and phrases: Extreme value distribution, Generalized Pareto distribution, Higher order asymptotic inference, Profile likelihood, Tangent exponential model

profile likelihood intervals are adequate overall, though small-sample bias appears for extrapolation too far into the tail. The improved methods yield wider confidence intervals with more accurate error rates, though slightly larger samples are needed for them to be effective. We illustrate the ideas by applying them to rainfall extremes in Venezuela, probabilities of severe flooding in Venice and excess lifetimes of Italian semi-supercentenarians.

2. Basic notions. Extreme value analysis is concerned with two main problems: estimating the probability of extremes of given sizes, and estimating a typical worst-case scenario over a given period. A standard approach is to fit specific distributions justified by asymptotic arguments to maxima (or minima) over specific time periods or to exceedances of a high (or low) threshold. The limiting distributions for high and low extremes are closely related, and we consider only maxima and exceedances of a high threshold.

2.1. Extremal distributions. The extremal types theorem (Fisher & Tippett, 1928; Gnedenko, 1943) characterizes the limiting distribution of maxima under mild conditions, but we use slightly stronger assumptions for ease of exposition. Let $F(x)$ denote a thrice-differentiable distribution function with density $f(x)$ whose support has upper endpoint x^* , define $s(x) = -F(x) \log\{F(x)\}/f(x)$, let b_m denote the solution of the equation $-\log F(b_m) = m^{-1}$ and let $a_m = s(b_m) > 0$. If M_m denotes the maximum of a block of m independent observations from F , then the existence of $\xi^* = \lim_{m \rightarrow \infty} s'(b_m)$ implies the existence of the limit

$$(2.1) \quad \lim_{m \rightarrow \infty} P\{(M_m - b_m)/a_m \leq x\} = \lim_{m \rightarrow \infty} F^m(a_m x + b_m) = \exp\left\{-(1 + \xi^* x)_+^{-1/\xi^*}\right\},$$

where $a_+ = \max(a, 0)$ for real a , and also implies convergence of both the corresponding density function and of its derivative uniformly in x on all finite intervals (Pickands, 1986, Theorem 5.2). Thus, if a_m and b_m were known, we might approximate the distribution of $(M_m - b_m)/a_m$ by the right-hand side of (2.1). In practice they are unknown, so we fit the generalized extreme value distribution $\text{GEV}(\mu, \sigma, \xi)$ with location parameter $\mu \in \mathbb{R}$, scale parameter $\sigma \in \mathbb{R}_+$ and shape parameter $\xi \in \mathbb{R}$,

$$(2.2) \quad G(x) = \begin{cases} \exp\left\{-\left(1 + \xi \frac{x - \mu}{\sigma}\right)^{-1/\xi}\right\}, & \xi \neq 0, \\ \exp\left\{-\exp\left(-\frac{x - \mu}{\sigma}\right)\right\}, & \xi = 0, \end{cases}$$

which is defined on $\{x \in \mathbb{R} : \xi(x - \mu)/\sigma > -1\}$. Setting $\xi = 0$ yields the Gumbel distribution. The $\text{GEV}(\mu, \sigma, \xi)$ is max-stable, and this allows extrapolation beyond the observed data into the tail of the distribution: if $X_i \sim \text{GEV}(\mu, \sigma, \xi)$ ($i = 1, \dots, T$) are independent, then $\max\{X_1, \dots, X_T\} \sim \text{GEV}(\mu_T, \sigma_T, \xi)$ with $\mu_T = \mu - \sigma(1 - T^\xi)/\xi$ and $\sigma_T = \sigma T^\xi$ when $\xi \neq 0$, and with $\mu_T = \mu + \sigma \log(T)$ and $\sigma_T = \sigma$ when $\xi = 0$. Thus if μ , σ and ξ have been estimated from n independent block maxima and the fit of the model appears adequate, then the distribution of a maximum of T further independent observations can also be estimated, even if $T \gg n$ — though the uncertainty generally grows alarmingly as T increases.

If eq. (2.1) holds, then the linearly rescaled conditional distribution of an exceedance over a threshold $u < x^*$ also converges (e.g., Embrechts et al., 1997, Theorem 3.4.5). Let $r(x) = \{1 - F(x)\}/f(x)$ denote the reciprocal hazard; then

$$(2.3) \quad \lim_{u \rightarrow x^*} \frac{1 - F\{u + r(u)x\}}{1 - F(u)} = 1 - H(x),$$

where

$$(2.4) \quad H(x) = \begin{cases} 1 - (1 + \xi x/\sigma)_+^{-1/\xi}, & \xi \neq 0, \\ 1 - \exp(-x/\sigma)_+, & \xi = 0, \end{cases}$$

is the generalized Pareto (GP) distribution function with scale $\sigma \in \mathbb{R}_+$ and shape $\xi \in \mathbb{R}$, denoted $\text{GP}(\sigma, \xi)$. If $X \sim \text{GP}(\sigma, \xi)$, straightforward calculations show that $X - u \mid X > u \sim \text{GP}(\sigma + \xi u, \xi)$ for any $u \in \mathbb{R}$ such that $\sigma + \xi u > 0$, so exceedances above a threshold u also follow a GP distribution. This property is termed threshold-stability, and its consequences parallel those of max-stability.

2.2. Risk measures. Max- and threshold-stability allow the estimation of risks associated with rare events. A common risk measure is the T -year return level, i.e., the quantile of F corresponding to an event of probability $p = 1 - 1/T$ for an annual maximum, often interpreted as “the level exceeded by an annual maximum on average once every T years”. The probability p_l that a T -year return level is exceeded l times over T years of independent annual maxima may be computed using a binomial distribution with T trials and success probability $1 - 1/T$. For large T , a Poisson approximation yields $p_0 = p_1 = 0.368$, $p_2 = 0.184$, $p_3 = 0.061$ and $p_4 = 0.015$, so the probability of at least one exceedance over T years is in fact roughly 0.63. The T -year return level approximates the 0.368 quantile of the distribution of the T -year maximum, leading Cox et al. (2002, § 3(b)) to suggest the use of direct summaries of this distribution instead of the return level. In the Bayesian paradigm, risk is typically associated with the prediction of future events using the posterior predictive distribution of the T -year maximum, which can be approximated by higher-order techniques (Davison, 1986).

We saw above that the distribution $G_T(x)$ of the maximum of T independent and identically distributed $\text{GEV}(\mu, \sigma, \xi)$ variates is $\text{GEV}(\mu_T, \sigma_T, \xi)$. Denote the expectation and p quantile of the T -year maximum by \mathfrak{e}_T and $\mathfrak{q}_p = G_T^{-1}(p)$ and the associated return level by $z_T = G^{-1}(1 - 1/T)$. These may all be expressed in the form

$$\begin{cases} \mu - \frac{\sigma}{\xi} (1 - \kappa_\xi), & \xi < 1, \xi \neq 0, \\ \mu + \sigma \kappa_0, & \xi = 0, \end{cases}$$

where κ_ξ equals $T^\xi \Gamma(1 - \xi)$ for \mathfrak{e}_T , $\{-T/\log(p)\}^\xi$ for \mathfrak{q}_p and $\{-\log(1 - 1/T)\}^{-\xi}$ for z_T , and κ_0 equals $\log(T) + \gamma_e$ for \mathfrak{e}_T , $\log(T) - \log\{-\log(p)\}$ for \mathfrak{q}_p and $-\log\{-\log(1 - 1/T)\}$ for z_T .

Threshold exceedances are related to maxima as follows: suppose we fit a $\text{GP}(\sigma_u, \xi)$ distribution to exceedances above a threshold u , and let ζ_u denote the unknown proportion of points above u . If there are on average n_y observations per year, then we take $H^{\zeta_u T n_y}$ as an approximation to the distribution of the T -year maximum above u .

2.3. Penultimate approximation. When the generalized extreme-value or generalized Pareto distribution is fitted to maxima or threshold exceedances, the best approximating extremal distribution depends on the block size m or threshold u and the shape parameters differ from their limiting values. Smith (1987) shows that, if $\xi^* = \lim_{m \rightarrow \infty} s'(b_m)$ exists,

then for any $x \in \{y : 1 + \xi^* y > 0\}$ there exists z such that

$$\frac{-\log[F\{v + s(v)x\}]}{-\log\{F(v)\}} = \{1 + s'(z)x\}^{-1/s'(z)}, \quad v < z < v + s(v)x.$$

For each $m \geq 1$, setting $v = b_m$ and $a_m = s(b_m)$ yields

$$F^m(a_m x + b_m) = \exp \left[- \{1 + s'(z)x\}^{-1/s'(z)} \right] + O(m^{-1}),$$

which can be regarded as a finite- m , or penultimate, version of the approximation stemming from eq. (2.1). Smith shows that the Hellinger distance between $F^m(a_m x + b_m)$ and the penultimate approximation $\text{GEV}\{0, 1, s'(b_m)\}$ approaches zero as $m \rightarrow \infty$ and that it is smaller than that between $F^m(a_m x + b_m)$ and $\text{GEV}(0, 1, \xi^*)$. Similar statements hold for the generalized Pareto distribution: unless $r'(x)$ is constant, there exists y such that a finite- u version of eq. (2.3),

$$\frac{1 - F\{u + r(u)x\}}{1 - F(u)} = \{1 + r'(y)x\}_+^{-1/r'(y)}, \quad u < y < u + r(u)x,$$

holds. One can replace the limiting shape $\lim_{v \rightarrow x^*} r'(v) = \xi^*$ by $r'(u)$, thereby reducing the Hellinger distance between the true conditional distribution of exceedances and the generalized Pareto approximation. Penultimate approximations for specific parametric models are straightforward to obtain, as one only needs to compute the scale a_m , location b_m and shape $s'(b_m)$ parameters for the GEV approximation or the scale $r(u)$ and shape $r'(u)$ parameters for the GP approximation.

When the limiting parametric models are fitted to finite samples, maximum likelihood estimates of the shape parameter will tend to be closer to their penultimate counterparts than to ξ^* ; moreover the estimator of ξ will converge to a target that changes as the threshold or the block size increases, depending on the curvature of s' or r' . Extrapolations far beyond the data will inevitably be biased due to the incorrect assumption that the max- or threshold-stability property that holds for infinite m or the limiting threshold also applies at finite levels.

2.4. Finite-sample bias. Although many approaches to estimation of the generalized Pareto and generalized extreme-value distribution have been proposed, we shall consider likelihood-based estimation, which has the advantages of being easily extended to the settings and sampling schemes that arise in our examples. The consistency and asymptotic normality of maximum likelihood estimators for the extremal distributions have been established (Bücher & Segers, 2017; Dombry & Ferreira, 2019, and references therein), but such studies consider infinite sample size, while small-sample biases can arise even when the assumed model is correct.

The finite-sample properties of maximum likelihood estimators for extreme value distributions can be poor (e.g., Hosking & Wallis, 1987, Table 5) due to their small-sample bias (Giles et al., 2016; Roodman, 2018). Figure 1 illustrates this for the shape parameter ξ . Apart from becoming more concentrated as the sample size n increases, the distribution of $\hat{\xi} - \xi$ when fitting the GEV distribution to maxima depends little on n , and in particular its median barely changes. The distribution of $\hat{\xi} - \xi$ based on the GP distribution shows strong negative skewness, with its median and lower quartile systematically increasing as n increases, while the upper quartile barely changes. There is a tradeoff between the resulting downward bias of $\hat{\xi}$ and upward bias of $\hat{\sigma}$ for GP samples, but quite apart from the penultimate effects described

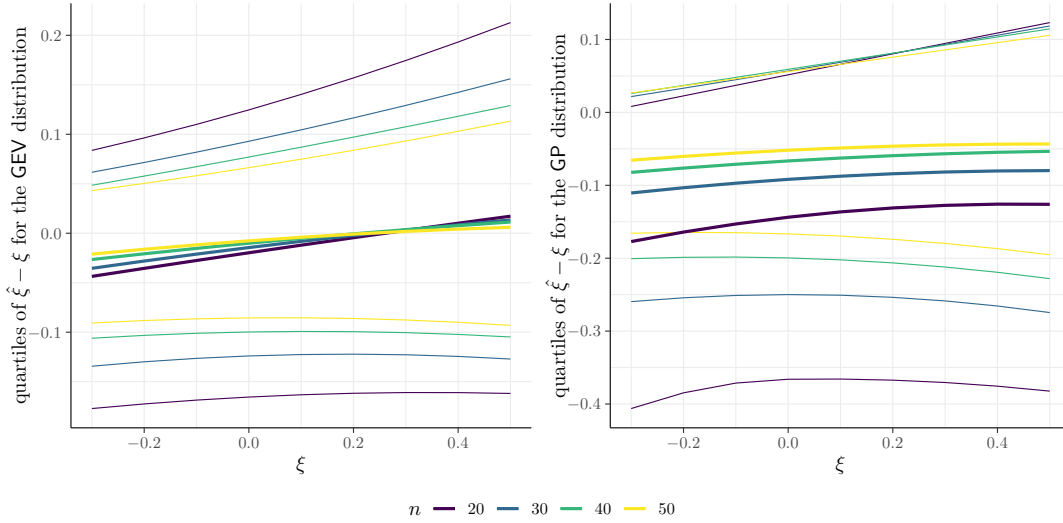


FIG 1. Smoothed quartiles of the distribution of differences between maximum likelihood estimates and true shape parameter, $\hat{\xi} - \xi$, based on 13000 simulations from $\text{GEV}(0, 1, \xi)$ and $\text{GP}(1, \xi)$ distributions for samples of sizes $n = 20, 30, 40, 50$.

above, extrapolation too far into the tail based on a GP fit tends to underestimate the sizes of extreme events. Bias-correction can mitigate this, but analytical first-order corrections of the type pioneered by Cox & Snell (1968) are applicable only when $\xi < -1/3$ and are unbounded near this. Analytical bias correction is quite different from bootstrap bias correction (Belzile, 2019) and furthermore bias-correction formulae for risk measures are currently unavailable. We thus consider implicit bias corrections below.

3. Improved likelihood inference. Consider a parametric model for observations y_1, \dots, y_n with log-likelihood function $\ell(\theta)$ whose p -dimensional parameter vector $\theta = (\psi, \lambda)$ can be decomposed into a q -dimensional parameter of interest ψ and a $(p - q)$ -dimensional nuisance vector λ . The score vector $U(\theta)$, the observed information matrix $j(\theta)$ and its inverse are partitioned accordingly and the maximum likelihood estimate is $\hat{\theta} = (\hat{\psi}, \hat{\lambda})$. The profile log-likelihood for the parameter of interest is

$$\ell_p(\psi) = \max_{\lambda} \ell(\psi, \lambda) = \ell(\hat{\theta}_\psi) = \ell(\psi, \hat{\lambda}_\psi).$$

The asymptotic properties of this and related statistics stem from those of the full likelihood and are standard under mild conditions (cf. Severini, 1999, p. 128): for example, if ψ is scalar with true value ψ_0 , the likelihood root

$$(3.1) \quad R(\psi_0) = \text{sign}(\hat{\psi} - \psi_0) [2\{\ell_p(\hat{\psi}) - \ell_p(\psi_0)\}]^{1/2}$$

has an asymptotic standard normal distribution to order $O(n^{-1/2})$. Confidence limits ψ_α for ψ are obtained by solving the equations $R(\psi_\alpha) = \Phi^{-1}(\alpha)$ for $\alpha \in (0, 1)$, with Φ denoting the standard normal cumulative distribution function. The same two-sided equi-tailed confidence intervals are obtained via χ^2 approximation to the distribution of the likelihood ratio statistic based on $\ell_p(\psi)$, but these and other first-order methods may perform badly in small samples if the dimension of λ is large, and higher-order methods may then provide more accurate tests and confidence intervals.

The standard asymptotic approximations described above apply under regularity conditions whereby the score statistic satisfies the first two Bartlett equalities. The r th moment of the score for the GEV and GP distributions exists only for $\xi > -1/r$ (Smith, 1985), so the above discussion applies to them only for $\xi > -1/2$. Estimates of ξ are rarely less than -0.3 in applications, and very often are close to zero, so the failure of regularity conditions is rarely of practical importance.

In the case of scalar ψ , one improvement is via normal approximation to a modified likelihood root (Barndorff-Nielsen & Cox, 1994, §6.6.1)

$$(3.2) \quad R^*(\psi) = R(\psi) + \frac{1}{R(\psi)} \log \left\{ \frac{Q(\psi)}{R(\psi)} \right\},$$

where $Q(\psi)$ is discussed below. If the response distribution is continuous, then $R^*(\psi_0)$ is asymptotically standard normal to order $O(n^{-3/2})$; this is known as a third-order approximation. In many ways more important than the reduction of the error rate from $n^{-1/2}$ to $n^{-3/2}$ is the fact that the error when using $R^*(\psi)$ is relative, leading to improved inferences even when $\hat{\psi}$ is distant from ψ_0 . Confidence limits are obtained by solving the equations $R^*(\psi_\alpha) = \Phi^{-1}(\alpha)$.

Estimators of ψ can be obtained by solving the equations $R(\psi) = 0$ and $R^*(\psi) = 0$. The first yields the maximum likelihood estimator $\hat{\psi}$, while the second, $\hat{\psi}^*$, yields an implicitly debiased version of $\hat{\psi}$. The maximum likelihood estimator could also be debiased directly by subtracting an estimated bias, or indirectly by modifying the corresponding score equation (Firth, 1993; Kenne Pagui et al., 2017; Belzile, 2019).

The use of eq. (3.2) hinges on the ready computation of $Q(\psi)$. This involves sample space derivatives of the log-likelihood, which are awkward in general, and a variety of approaches to their computation have been proposed. In the next section we sketch a simple general approach developed by D. A. S. Fraser, N. Reid and colleagues.

3.1. Tangent exponential model. The tangent exponential (TEM) model provides a general formula for the quantity $Q(\psi)$ that appears in eq. (3.2) (Fraser et al., 1999). The idea is to approximate the probability density function of the data by that of an exponential family, for which highly accurate inference is possible. Following Brazzale et al. (2007, Chapter 8), we outline its construction. The presence of sample space derivatives makes it necessary to distinguish a generic response vector $\mathbf{y} = (y_1, \dots, y_n)^\top$ from the responses actually observed, $\mathbf{y}^o = (y_1^o, \dots, y_n^o)^\top$.

The tangent exponential model depends on an $n \times p$ matrix \mathbf{V} , whose i th row equals the derivative of y_i with respect to $\boldsymbol{\theta}^\top$, evaluated at $\hat{\boldsymbol{\theta}}$ and \mathbf{y}^o ; the p columns of \mathbf{V} correspond to vectors in \mathbb{R}^n that are informative about the variation of \mathbf{y} with $\boldsymbol{\theta}$. The TEM implicitly conditions on an $(n - p)$ -dimensional approximate ancillary statistic whose value lies in the space orthogonal to the columns of \mathbf{V} , and constructs a local exponential family approximation at $\hat{\boldsymbol{\theta}}$ and \mathbf{y}^o with canonical parameter

$$\boldsymbol{\varphi}(\boldsymbol{\theta}) = \mathbf{V}^\top \left. \frac{\partial \ell(\boldsymbol{\theta}; \mathbf{y})}{\partial \mathbf{y}} \right|_{\mathbf{y}=\mathbf{y}^o}.$$

The components of $\boldsymbol{\varphi}(\boldsymbol{\theta})$ can be interpreted as the directional derivatives of $\ell(\boldsymbol{\theta}; \mathbf{y}^o + \mathbf{V}\mathbf{t})$ with respect to the columns of \mathbf{V} , obtained by differentiating with respect to the components of the $p \times 1$ vector \mathbf{t} and setting $\mathbf{t} = \mathbf{0}$.

In models for continuous scalar responses the \mathbf{V}_i can be obtained by using the probability integral transform to write $y_i = F^{-1}(u_i; \boldsymbol{\theta})$ in terms of a uniform variable u_i , yielding

$$(3.3) \quad \mathbf{V}_i = \frac{\partial y_i}{\partial \boldsymbol{\theta}^\top} \bigg|_{\mathbf{y}=\mathbf{y}^o, \boldsymbol{\theta}=\hat{\boldsymbol{\theta}}} = - \frac{\partial F(y_i^o; \boldsymbol{\theta})}{\partial \boldsymbol{\theta}^\top} \frac{1}{f(y_i^o; \boldsymbol{\theta})} \bigg|_{\boldsymbol{\theta}=\hat{\boldsymbol{\theta}}}, \quad i = 1, \dots, n;$$

equivalently we may take the total derivative of the pivotal quantity $F(y_i; \boldsymbol{\theta})$. Discrete responses cannot be differentiated in the same way and are replaced by their means, leading to an error of order n^{-1} for inferences based on eq. (3.2) (Davison et al., 2006).

The approximate pivot in eq. (3.2) stemming from the TEM is

$$(3.4) \quad Q(\psi) = \frac{\left| \boldsymbol{\varphi}(\hat{\boldsymbol{\theta}}) - \boldsymbol{\varphi}(\hat{\boldsymbol{\theta}}_\psi) \quad \partial \boldsymbol{\varphi} / \partial \boldsymbol{\lambda}^\top(\hat{\boldsymbol{\theta}}_\psi) \right|}{\left| \partial \boldsymbol{\varphi} / \partial \boldsymbol{\theta}^\top(\hat{\boldsymbol{\theta}}) \right|} \frac{\left| j(\hat{\boldsymbol{\theta}}) \right|^{1/2}}{\left| j_{\lambda\lambda}(\hat{\boldsymbol{\theta}}_\psi) \right|^{1/2}},$$

where the first matrix in the numerator is formed by binding the $p \times 1$ vector $\boldsymbol{\varphi}(\hat{\boldsymbol{\theta}}) - \boldsymbol{\varphi}(\hat{\boldsymbol{\theta}}_\psi)$ with the $p \times (p-1)$ matrix $\partial \boldsymbol{\varphi} / \partial \boldsymbol{\lambda}^\top$. A modified profile likelihood $\ell_{\text{fr}}(\psi) = -\{R^*(\psi)\}^2/2$ may be constructed by using eq. (3.4) and treating $R^*(\psi)$ as standard normal.

3.2. Modified profile likelihoods. In the previous section, the likelihood root was derived from the profile log-likelihood function via the likelihood ratio statistic, then modified and used to construct the modified profile likelihood $\ell_{\text{fr}}(\psi)$. An alternative is direct modification of the profile log-likelihood, two approaches to which are listed by Severini (2000, § 9). The first approach uses elements of the tangent exponential model and is of the form

$$(3.5) \quad \ell_{\text{m}}^{\text{tem}}(\psi) = \ell_{\text{p}}(\psi) + \frac{1}{2} \log \left\{ \left| j_{\lambda\lambda}(\hat{\boldsymbol{\theta}}_\psi) \right| \right\} - \log \left\{ \left| \ell_{\lambda; \mathbf{y}}(\hat{\boldsymbol{\theta}}_\psi) \mathbf{V}_\lambda(\hat{\boldsymbol{\theta}}) \right| \right\},$$

where $\ell_{\lambda; \mathbf{y}} = \partial^2 \ell / \partial \boldsymbol{\lambda} \partial \mathbf{y}^\top$ is the derivative of the log-likelihood with respect to the nuisance parameter and observations and \mathbf{V}_λ denotes the columns of \mathbf{V} in eq. (3.3) corresponding to derivatives with respect to $\boldsymbol{\lambda}$. The second approach, due to Severini and similar in spirit to ideas in Skovgaard (1996), uses empirical covariances, yielding

$$(3.6) \quad \ell_{\text{m}}^{\text{cov}}(\psi) = \ell_{\text{p}}(\psi) + \frac{1}{2} \log \left\{ \left| j_{\lambda\lambda}(\hat{\boldsymbol{\theta}}_\psi) \right| \right\} - \log \left\{ \left| \hat{i}_{\lambda; \lambda}(\hat{\boldsymbol{\theta}}_\psi; \hat{\boldsymbol{\theta}}) \right| \right\},$$

where

$$\hat{i}_{\lambda; \lambda}(\hat{\boldsymbol{\theta}}_\psi; \hat{\boldsymbol{\theta}}) = \sum_{i=1}^n \ell_{\lambda}^{(i)}(\hat{\boldsymbol{\theta}}_\psi) \ell_{\lambda}^{(i)}(\hat{\boldsymbol{\theta}})^\top;$$

here $\ell_{\lambda}^{(i)}$ denotes the component of the score statistic due to the i th observation.

We illustrate the derivation of the above quantities by two examples.

EXAMPLE 1 (Modified profile likelihood for the scale of maxima). Consider independent and identically distributed observations $Y_i \sim \text{GEV}(\mu, \sigma, \xi)$ ($i = 1, \dots, n$) with $\psi = \sigma$ and $\boldsymbol{\lambda} = (\mu, \xi)$. The i th row of the matrix \mathbf{V} has elements

$$V_{i, \mu} = 1, \quad V_{i, \sigma} = (y_i^o - \hat{\mu}) / \hat{\sigma}, \quad V_{i, \xi} = \frac{\hat{\sigma} s_i(\hat{\boldsymbol{\theta}}) \log\{s_i(\hat{\boldsymbol{\theta}})\}}{\hat{\xi}^2} - \frac{y_i^o - \hat{\mu}}{\hat{\xi}},$$

where $s_i(\boldsymbol{\theta}) = \{1 + \xi(y_i^o - \mu)/\sigma\}$. The form of $V_{i,\mu}$ and $V_{i,\sigma}$ would be the same for any location-scale model, whereas $V_{i,\xi}$ is specific to the generalized extreme-value distribution. The sample space derivatives appearing in eq. (3.5),

$$\begin{aligned}\ell_{\mu,y_i}(\hat{\boldsymbol{\theta}}_\sigma) &= \frac{1 + \hat{\xi}_\sigma}{\sigma^2} s_i(\hat{\boldsymbol{\theta}}_\sigma)^{-1/\hat{\xi}_\sigma - 2} - \frac{\hat{\xi}_\sigma(1 + \hat{\xi}_\sigma)}{\sigma^2 s_i(\hat{\boldsymbol{\theta}}_\sigma)^2}, \\ \ell_{\xi,y_i}(\hat{\boldsymbol{\theta}}_\sigma) &= \frac{s_i(\hat{\boldsymbol{\theta}}_\sigma)^{-1/\hat{\xi}_\sigma - 1}}{\sigma} \left(\frac{(y_i^o - \hat{\mu}_\sigma)(1 + \hat{\xi}_\sigma)}{\sigma \hat{\xi}_\sigma s_i(\hat{\boldsymbol{\theta}}_\sigma)} + \frac{\log\{s_i(\hat{\boldsymbol{\theta}}_\sigma)\}}{\hat{\xi}_\sigma^2} \right) \\ &\quad + \frac{1}{\sigma s_i(\hat{\boldsymbol{\theta}}_\sigma)} + \frac{(1 + \hat{\xi}_\sigma)(y_i^o - \hat{\mu}_\sigma)}{\sigma^2 s_i(\hat{\boldsymbol{\theta}}_\sigma)^2},\end{aligned}$$

depend on the maximum likelihood estimates $\hat{\boldsymbol{\theta}}_\sigma = (\hat{\mu}_\sigma, \sigma, \hat{\xi}_\sigma)$ for fixed σ , and are then used to obtain the modified profile log-likelihood ℓ_m^{tem} .

EXAMPLE 2 (Expected maximum of N threshold exceedances). Consider modelling threshold exceedances above u with a generalized Pareto distribution (2.4) in order to make inference on the expected maximum of N exceedances,

$$\mathfrak{z}_N := \int_0^\infty z N F(z)^{N-1} f(z) dz = \frac{\sigma}{\xi} \left\{ \frac{\Gamma(N+1)\Gamma(1-\xi)}{\Gamma(N+1-\xi)} - 1 \right\}, \quad \xi < 1.$$

We parametrize the likelihood in terms of (\mathfrak{z}_N, ξ) , in which case the $n_u \times 2$ matrix \mathbf{V} appearing in the tangent exponential model has elements $V_{i,\mathfrak{z}_N} = x_i/\mathfrak{z}_N$, and

$$V_{i,\xi} = \frac{\hat{\xi} N \text{Be}(N, 1 - \hat{\xi}) \left\{ \psi^{(0)}(1 - \hat{\xi}) - \psi^{(0)}(N + 1 - \hat{\xi}) \right\} x_i - \hat{\mathfrak{z}}_N \hat{\mathfrak{q}}_i \log(\hat{\mathfrak{q}}_i)}{\hat{C} \hat{\xi}},$$

where $\psi^{(0)}(x) = \Gamma'(x)/\Gamma(x)$ is the digamma function, $\text{Be}(a, b) = \int_0^1 t^{a-1}(1-t)^{b-1} dt$ is the Beta function, x_1, \dots, x_{n_u} are the observations that exceed the threshold u and

$$\mathfrak{q}_i = 1 + C \left(\frac{x_i}{\mathfrak{z}_N} \right), \quad C = N \text{Be}(N, 1 - \xi) - 1,$$

with $\hat{\mathfrak{q}}_i$ and \hat{C} denoting instances of these functions evaluated at the maximum likelihood estimate. The canonical parameter $\boldsymbol{\varphi}(\xi, \mathfrak{z}_N)$ equals

$$\sum_{i=1}^{n_u} \boldsymbol{\varphi}_i = - \sum_{i=1}^{n_u} \mathbf{V}_i \times \left(1 + \frac{1}{\xi} \right) [(\mathfrak{z}_N - u)C + (x_i - u)]^{-1}, \quad i = 1, \dots, n_u,$$

and the mixed partial derivatives appearing in eq. (3.4) are

$$\begin{aligned}\frac{\partial \boldsymbol{\varphi}_i}{\partial \xi} &= \mathbf{V}_i \times \left[\left(1 + \frac{1}{\xi} \right) \frac{C \{ \psi(1 - \xi) - \psi(N + 1 - \xi) \}}{\mathfrak{z}_N^2 \mathfrak{q}_i^2} (\mathfrak{z}_N \mathfrak{q}_i - C x_i) - \frac{C}{\xi^2 \mathfrak{z}_N \mathfrak{q}_i} \right], \\ \frac{\partial \boldsymbol{\varphi}_i}{\partial \mathfrak{z}_N} &= \mathbf{V}_i \times \left(1 + \frac{1}{\xi} \right) \frac{C(\mathfrak{z}_N - C x_i)}{\mathfrak{z}_N^3 \mathfrak{q}_i}.\end{aligned}$$

The components of the score vectors and information matrices are readily obtained, if necessary using computer algebra, though care is needed to interpolate them for the GEV at $\xi = 0$.

4. Simulation study. We used Monte Carlo simulation to investigate small-sample inference for risk measures based on the profile log-likelihood, the tangent exponential model approximation and Severini’s corrections.

Sample sizes for extremes, whether block maxima or threshold exceedances, are often small. For example, one may attempt to predict the 100-year maximum temperature based on 20 years of daily records, where restricting attention to summer months yields around 90 observations per year. To mimic this scenario, we generated 1800 independent observations from a parametric model and targeted the expectation and median of the distribution of 9000-observation maximum from that same distribution, with benchmarks computed using penultimate approximations.

The choice of block size or threshold compromises between closeness of approximation (and thus reduced asymptotic bias) and small-sample effects. For larger block size/thresholds, the extreme-value approximation is in principle better, but estimation uncertainty is larger because of the smaller sample size. We divided the 1800 simulated values into blocks of sizes $m = 30, 45, 90$, and fitted the GEV distribution to the block maxima. We also fitted the GP distribution to the largest $n_u = 20, 40, 60$ order statistics of a sample of size 1800 from the GP distribution. We likewise generated data from six other distributions mentioned in Section 2.3 and applied both block maximum and threshold methods to these data; see the Supplementary Material.

For each sample, we obtained four estimates and five sets of confidence limits for ψ , based on the Wald statistic; the likelihood root $R(\psi)$ and the modified likelihood root $R^*(\psi)$ defined in eq. (3.1) and eq. (3.2); and the modified profile likelihoods (3.5) and (3.6). The Wald statistic was computed on the log scale and back-transformed, i.e., with limits $\exp\{\log(\hat{\psi}) \pm \Phi^{-1}(1 - \alpha/2) \text{se}(\hat{\psi})/\hat{\psi}\}$; the log transformation is intended to mitigate the poor properties of this statistic in highly asymmetric situations. For each target (return level, median and expectation of the T -year maximum), distribution and threshold or block size, we also calculated the relative bias of the point estimators, and the overall coverage and the average widths of two-sided confidence intervals. The full results are in the Supplementary Material, and we summarise the main findings below, focusing on properties of one-sided confidence limits.

4.1. Summary of findings.

Relative error of one-sided confidence intervals. Figures 2 and 3 display one-sided relative coverage errors for the expected N -observation maximum; similar results hold for N -observation median and N -observation return level. Despite the log-transformation, the Wald intervals fail to capture the positive skewness of the estimators of z_N , $q_{1/2}$ (not shown) and ϵ_N defined in Section 2.2. The one-sided relative coverage error for the Wald statistics are so poor that they fall outside the limits of Figures 2 and 3: for example, applying the block maximum method with 20 observations to samples from a GEV distribution (Table 5), the 99% Wald-based confidence intervals contain the true value roughly 85% of the time when $\xi = 0.1$ and 81% of the time when $\xi = -0.1$, but the 5% empirical error rate for the lower limit is 0%, indicating that the interval is too wide on the left and much too short on the right.

If the data are generated from the generalized extreme value distribution, the empirical error rates for the TEM are closer to nominal, but no method is universally better. Perhaps unexpectedly, the penultimate effects are not really visible for the other distributions (Table 5).

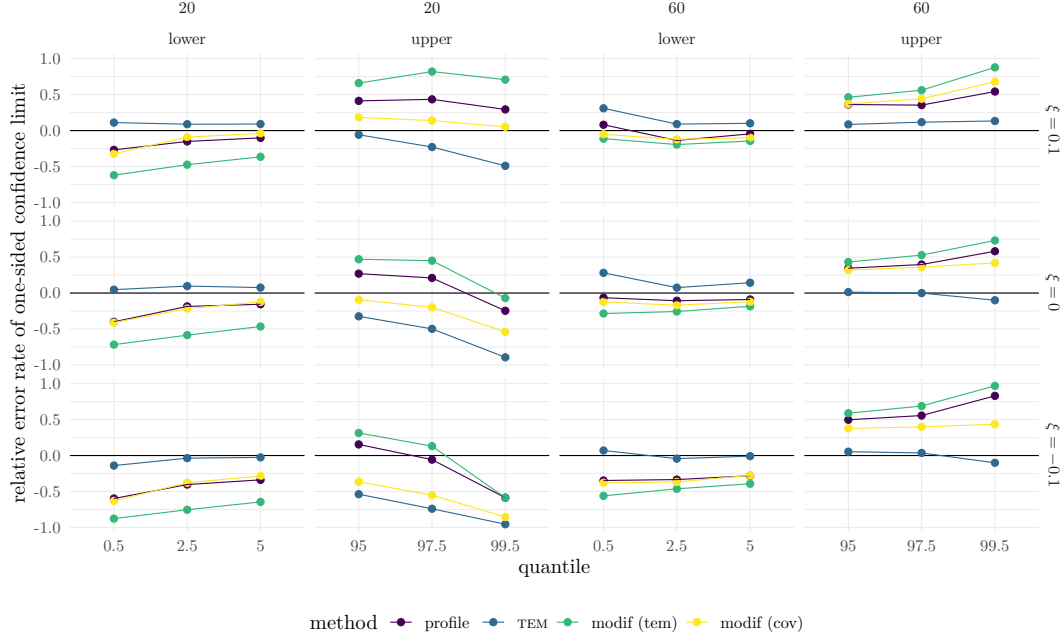


FIG 2. Relative coverage errors for one-sided lower and upper confidence limits with nominal error rates 0.5%, 2.5% and 5% for the expected 9000-observation maximum estimated using maxima of generalized extreme value samples of sizes $n = 20$ (left) and $n = 60$ (right) with shape parameter $\xi = -0.1, 0, 0.1$ (bottom to top). An ideal method would have zero relative error in both tails, whereas methods with relative error ± 0.5 have empirical error rates 1.5 (+) or 0.5 (−) times the nominal rate. The upper and lower tail errors for intervals whose relative errors have opposite signs will cancel to some extent when a two-sided interval is computed. If both upper and lower tail errors are positive, the corresponding two-sided intervals have empirical coverage that is too low, whereas negative upper and lower tail errors correspond to conservative two-sided confidence intervals.

The profile and higher-order methods for block maxima seem impervious to the effects of extrapolation and their coverage is excellent overall.

Figure 3 shows that the results based on threshold exceedances are more variable. The performance of Wald-based intervals remains calamitous: the empirical upper error rate for the nominal 5% limit is close to 30% in all scenarios for the untransformed Wald statistic and improves only to 20–30% after transformation. With $k = 20$ observations (Figure 3 and table 7), most higher-order methods overcover even when the model is correctly specified. The TEM interval is shifted to the right, whereas Severini’s corrections display higher empirical error in the lower tail. This breakdown of the TEM could be attributed to penultimate effects and small sample bias, as it vanishes as the sample size grows; the TEM performs very well when $k = 60$ (Table 6). Two-sided profile likelihood intervals typically have good coverage, but their upper empirical error rates can be more than double the nominal values, as the intervals tend to lie too far to the left. Thus the price paid for improved intervals with better coverage is increased uncertainty stemming from their greater width.

Width of confidence intervals. The expected N -observation maximum is larger than both the median of the N -observation maximum and the N -year return level when $\xi > 0$, and its confidence intervals are the widest of those for all three risk measures due to the extrapolation in the upper tail. The higher-order intervals, especially those based on R^* , overcover slightly

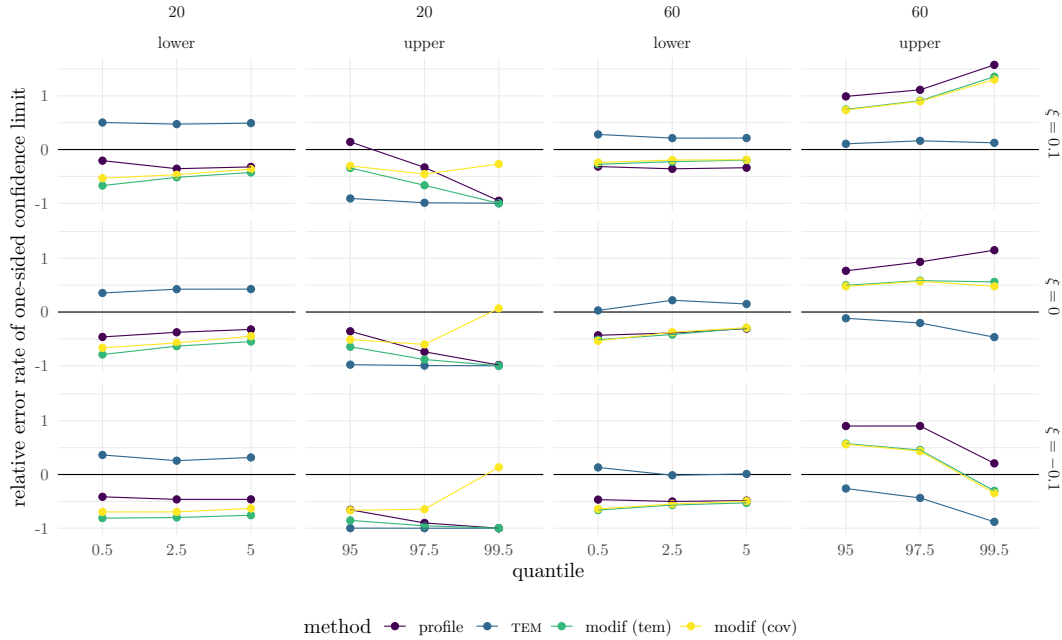


FIG 3. Relative coverage errors for one-sided lower and upper confidence limits for the expected 9000-observation maximum estimated using generalized Pareto samples of sizes $n = 20$ (left) and $n = 60$ (right) with $\xi = -0.1, 0, 0.1$ (bottom to top). See the caption to Figure 2 for explanation.

when the sample size is smaller and the blocks are larger, e.g., for $m = 90$ with $k = 20$ (Table 5). The average widths of two-sided confidence intervals for the block maximum method with $m = 30$, $k = 60$ are comparable (not shown). For this setting, the intervals based on ℓ_m^{tem} are the shortest among those implemented.

Higher-order methods for threshold exceedances give wider confidence intervals, often because they have better coverage in the upper tail: for example, the TEM confidence intervals are between 1.75 and 2 times wider than those based on the profile likelihood when $k = 20$ and about 1.25 times wider when $k = 60$.

Bias of point estimators of risk measures. When using threshold exceedances, maximum likelihood estimators of ξ are negatively biased for any sample size $k \leq 60$ (Figure 1) and risk estimators are likewise downwardly biased. For $k = 20$, the TEM point estimators obtained by solving the equation $R^*(\psi) = 0$ are positively biased, but they have the lowest bias of all point estimators considered when $k \geq 40$. The point estimators derived using Severini's modified profile log-likelihoods have lower bias than the maximum likelihood estimator.

4.2. Practical guidelines. Wald-based confidence intervals should never be used; their coverage is appallingly low, even after transformation. For block maxima, profile likelihood-based confidence intervals have good two-sided coverage overall for the risk measures we considered, and there seems to be little gain in using higher-order methods: the discrepancy between the empirical error rates in the lower and upper tails seems to be due to the bias of the risk estimators themselves. For both types of data, the TEM-based estimator is systematically larger than the maximum likelihood estimator. For threshold exceedances, TEM-based

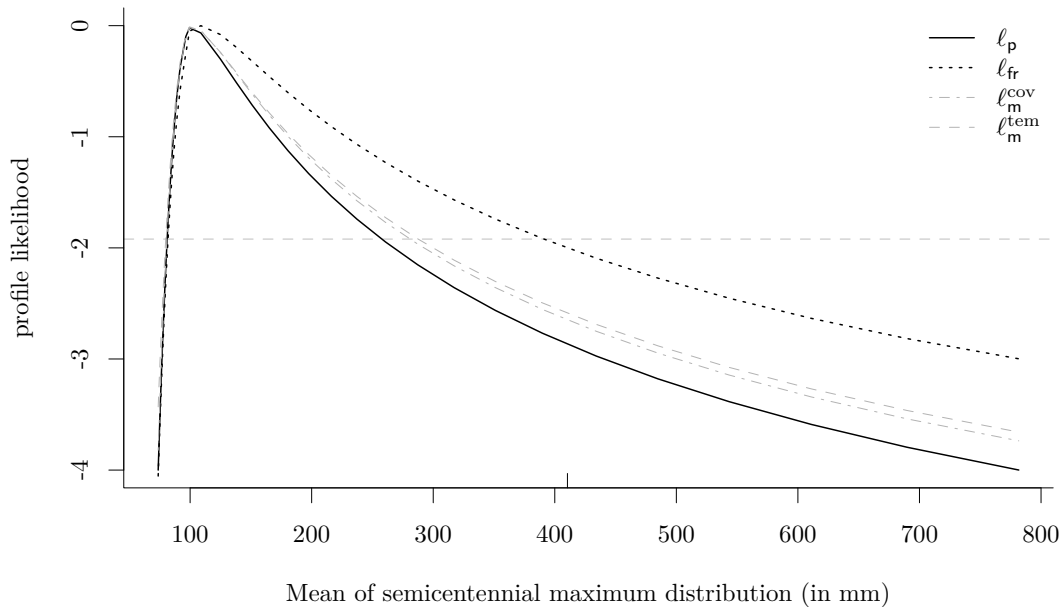


FIG 4. Weighted profile likelihood and higher-order versions for the expected semicentennial maximum daily rainfall at Maiquetía based on threshold exceedances above 27mm, using daily data from 1961–1998. Profile likelihood (full black line), tangent exponential model approximation (dotted) and Severini’s modified profiles (grey dashed and dot-dashed). The dashed grey horizontal line at -1.92 indicates cutoff values for 95% confidence intervals based on the asymptotic χ^2_1 distribution. The mark at 410.4mm indicates the record of December 15th, 1999.

confidence intervals have very good coverage and the corresponding point estimators have smaller bias when the sample size is larger than around 50; while no higher-order method is always better, TEM-based intervals usually improve on the others.

5. Data illustrations.

5.1. *Vargas tragedy.* Cumulative rainfall of around 911mm over a three-day period in mid-December 1999 led to landslides and debris flow that caused an estimated 30,000 deaths in the coastal Venezuelan state of Vargas. In addition to yearly maximum daily rainfall for the period 1951–1960, daily cumulated rainfall data (mm) recorded at the Maiquetía *Simón Bolívar International Airport* are available for 1961–1999. These data were analyzed in Coles & Pericchi (2003) and Coles et al. (2003), whose initial fit to annual maxima up to 1998 suggested that the return period for such an event would be approximately 18 million years, though more sophisticated models led to much more reasonable risk estimates.

To illustrate the effect of improved likelihood approximations, we use a generalized Pareto model for the tail of daily cumulated rainfall for 1961–1998. Standard diagnostic plots suggest that taking the threshold u above 25mm is reasonable, but inference is very sensitive to the choice of u , owing to the large number of events in the range 45–55mm. Although the estimate of ξ decreases steadily as u increases, the additional uncertainty due to the decrease in sample size n_u makes the the largest daily observed event of 410.4mm more likely.

The month of December is typically dry in Vargas, with occasional intense rainfall episodes. Retaining all the observations may confound meteorological events of different

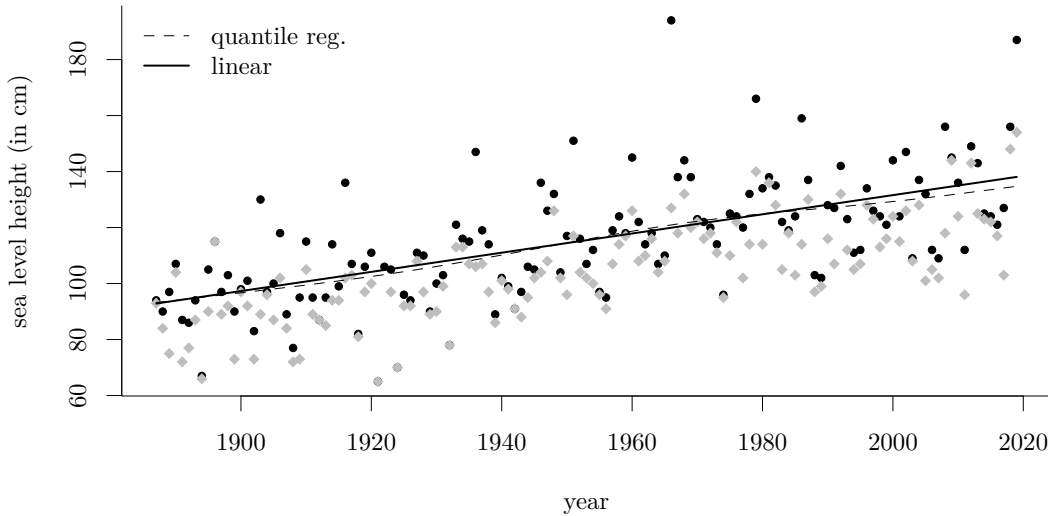


FIG 5. First (black) and second (grey) largest yearly observations for the Venice sea level data (in cm), a smooth additive quantile regression model for the median (with a smooth term for time and a different intercept for each order statistic). The predicted values for the largest order statistic and those for the corresponding linear regression are superimposed.

types, so we attempt to allow for this by weighting the log likelihood contributions using the kernel $w(t - t_i) = \exp[\nu \cos\{2\pi(t - t_j)/365\} - \nu]$, where t_j is the day of the year in which an exceedance occurred, t is December 15th and ν is a concentration parameter. We set a threshold to the 0.96 quantile of the empirical distribution of non-zero rainfall up to 1998, i.e., $u = 27\text{mm}$, which leaves 145 observations; with $\nu = 4$, the effective sample size is the sum of weights, which is 35. The likelihood methods are easily modified to allow for this, and the profile log likelihoods are displayed in Figure 4. The point estimates of the expected 50-year maximum are all around 100mm, but the 95% confidence interval based on the TEM, $[82.3, 391]\text{mm}$, is much wider than that based on the profile likelihood, $[81.3, 259]\text{mm}$, suggesting that the largest daily value seen in 1961–1999 is not unlikely once small-sample effects are taken into account.

5.2. Venice sea level. The Italian city of Venice is threatened by sea-level rise and subsidence, and is increasingly at risk from flooding in so-called *acqua alta* events. To quantify this risk we consider data analyzed by Smith (1986) and Pirazzoli (1982) containing large annual sea level measurements from 1887 until 1981, complemented with series for 1982–2019 extracted from the City of Venice website (accessed June 2020 and available under the CC BY-NC-SA 3.0 license). Only the yearly maximum is available for 1922 and only the six largest observations for 1936. Figure 5 shows the two largest annual order statistics; while there is a clear trend due to sea level rise, we detected no change when the measurement gauge was relocated in 1983. In addition to a simple straight-line model we fitted a smooth additive nonparametric quantile regression (Fasiolo et al., 2020) with 50 knots with a smooth term for years and different intercepts for the two largest order statistics: the resulting fits are plotted in Figure 5 and suggest that a straight line is adequate.

If the extremal types theorem holds, then the log-likelihood of the limiting distribution of the r largest observations of a sample, $Y_{(1)} \geq \dots \geq Y_{(r)}$, is

$$\begin{aligned} \ell(\mu, \sigma, \xi; \mathbf{y}) = & -r \log(\sigma) - \left(1 + \frac{1}{\xi}\right) \sum_{j=1}^r \log \left(1 + \xi \frac{y_{(j)} - \mu}{\sigma}\right)_+ \\ & - \left(1 + \xi \frac{y_{(r)} - \mu}{\sigma}\right)_+^{-1/\xi}, \quad \mu, \xi \in \mathbb{R}, \sigma > 0. \end{aligned}$$

In the analysis below we use these log-likelihood contributions with the $r = 2$ largest observations for each year and treat data for different years as independent. The quality of the asymptotic approximation degrades quickly when r increases, and diagnostic plots suggest that just two extrema each year should be used. Our chosen risk measure is the probability that in year t the annual maximum sea level exceeds the level $z = 194\text{cm}$ reached in the catastrophic flooding of 1966, based on a non-stationary extremal model with parameters $\mu_0 + \mu_1 \mathbf{y} \in \mathbb{R}$, σ and ξ .

In order to compute the terms necessary for the TEM approximation, suppose that we have data (y_1, \dots, y_r) and pivots

$$u_1(y_1; \boldsymbol{\theta}), \quad u_2(y_1, y_2; \boldsymbol{\theta}), \quad \dots, \quad u_r(y_1, \dots, y_r; \boldsymbol{\theta}).$$

Total differentiation of $u_1(y_1; \boldsymbol{\theta})$ with respect to y_1 and $\boldsymbol{\theta}$ yields

$$0 = \frac{\partial u_1(y_1; \boldsymbol{\theta})}{\partial \boldsymbol{\theta}} + \frac{\partial y_1}{\partial \boldsymbol{\theta}} \frac{\partial u_1(y_1; \boldsymbol{\theta})}{\partial y_1},$$

and therefore

$$\frac{\partial y_1}{\partial \boldsymbol{\theta}} = - \left\{ \frac{\partial u_1(y_1; \boldsymbol{\theta})}{\partial y_1} \right\}^{-1} \frac{\partial u_1(y_1; \boldsymbol{\theta})}{\partial \boldsymbol{\theta}}.$$

Total differentiation of $u_j(y_1, \dots, y_j; \boldsymbol{\theta})$ with respect to y_1, \dots, y_j and $\boldsymbol{\theta}$ likewise yields

$$\frac{\partial y_j}{\partial \boldsymbol{\theta}} = - \left\{ \frac{\partial u_j(y_1, \dots, y_j; \boldsymbol{\theta})}{\partial y_j} \right\}^{-1} \left\{ \frac{\partial u_j(y_1, \dots, y_j; \boldsymbol{\theta})}{\partial \boldsymbol{\theta}} + \sum_{i=1}^{j-1} \frac{\partial y_i}{\partial \boldsymbol{\theta}} \frac{\partial u_i(y_1, \dots, y_i; \boldsymbol{\theta})}{\partial y_i} \right\},$$

with all these expressions evaluated at y_1^o, \dots, y_j^o and $\hat{\boldsymbol{\theta}}$.

In the present case the pivots stem from the Poisson process representation

$$0 < \Lambda_{\boldsymbol{\theta}}(y_1) < \Lambda_{\boldsymbol{\theta}}(y_2) < \dots < \Lambda_{\boldsymbol{\theta}}(y_r), \quad \Lambda_{\boldsymbol{\theta}}(y) = \{1 + \xi(y - \mu)/\sigma\}_+^{-1/\xi},$$

whereby the standard exponential differences $\Lambda_{\boldsymbol{\theta}}(y_j) - \Lambda_{\boldsymbol{\theta}}(y_{j-1})$ are pivotal. The expressions above simplify, as the $u_j(y_1, \dots, y_j; \boldsymbol{\theta}) = \Lambda_{\boldsymbol{\theta}}(y_j) - \Lambda_{\boldsymbol{\theta}}(y_{j-1})$ involve at most two of the y_i .

Figure 6 shows that the profile- and TEM-based point estimates and 95% confidence intervals for the probability of a flood exceeding the 1966 level for various years are quite similar, though the higher-order estimates vary slightly more over time. Despite the increase in sea level, it appears that an event as rare as that in 1966 will remain unlikely for at least the next two decades.

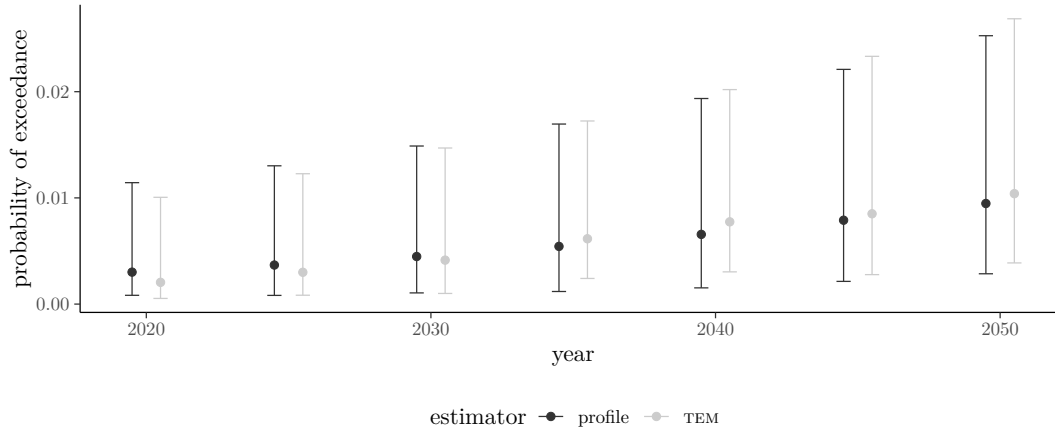


FIG 6. Probability of exceedance of 194cm with 95% pointwise confidence intervals as a function of the year, based on the profile likelihood (blue) and the modified likelihood root R^* (grey).

5.3. Old age in Italy. The existence or not of a finite upper limit for human lifetimes has recently sparked interest in the extreme value community (Hanayama & Sibuya, 2016; Rootzén & Zholud, 2017; Einmahl et al., 2019). The Italian centenarian data set, kindly provided by Holger Rootzén, contains the birth dates and ages of 3836 individuals from a study of semi-supercentenarians conducted by the Istituto Nazionale di Statistica (Istat); see Barbi et al. (2018). Individuals in the dataset if they were aged 105 years or more at some point between January 1st, 2009 (c_1) and January 1st, 2016 (c_2); the survival time is censored for individuals alive at c_2 . The cohort comprises persons born between 1896 and 1910 with excess lifetimes above 105 years measured in days above $u = 38351$ days. It is natural to fit the generalized Pareto model to these excess lifetimes, but it is important to account for the potential left-truncation and right-censoring. Failure to account for the censoring would lead to negative bias for the shape parameter ξ , for example, since individuals born after 1910 could not attain 116 years. A negative shape parameter corresponds to a finite upper limit $\iota = -\sigma/\xi$, whereas $\xi \geq 0$ means there is no upper limit.

We consider excess lifetime of individuals whose age exceeded u between calendar times c_1 and c_2 : let S and f denote the survival and the density functions of lifetimes, let x_i denote the calendar date at which individual i reached u years, let t_i denote the excess lifetime above u at calendar time c_2 , and let a_i be an indicator variable taking value 1 if individual i was alive at calendar time c_2 and zero otherwise. Then the likelihood is

$$L(\theta; \mathbf{t}, \mathbf{s}) = \prod_{i=1}^n \left[\frac{f(t_i)}{S\{(c_1 - x_i)_+\}} \right]^{1-a_i} \left[\frac{S(t_i)}{S\{(c_1 - x_i)_+\}} \right]^{a_i},$$

with the first and second terms corresponding to those individuals seen to die and to those whose lifetimes are censored at c_2 . We fit a generalized Pareto distribution to excess lifetimes over a range of thresholds starting from 105 years and report the maximum likelihood estimates of the parameters in Table 1. The largest excess lifetime, for Emma Moreno, who died aged 117 years in 2017, after c_2 , is censored, and the estimated shape $\hat{\xi}_u$ for threshold u is typically close to zero, although its variability is large for high u .

u	n_u	$\hat{\sigma}$	$\hat{\xi}$	$\ell(\hat{\theta})$
105	3836	1.67 (0.04)	-0.04 (0.02)	-4253.7
106	1874	1.70 (0.06)	-0.07 (0.03)	-2064.3
107	946	1.47 (0.08)	-0.02 (0.04)	-999.3
108	415	1.47 (0.11)	-0.01 (0.06)	-440.6
109	198	1.33 (0.15)	0.03 (0.09)	-202.9
110	88	1.22 (0.23)	0.12 (0.17)	-85.4
111	34	1.50 (0.47)	0.06 (0.30)	-34.9

TABLE 1

Maximum likelihood estimates of the generalized Pareto for the Italian super-centenarian data. From left to right, threshold u (in years), number of threshold exceedances n_u , estimates (standard errors) of the scale σ , shape ξ parameters, log-likelihood at MLE $\ell(\hat{\theta})$.

u	R	R^*
105	142.2 (128.5, 213.7)	143.6 (129.3, 235.3)
105.5	127.5 (122.1, 138.5)	127.7 (122.3, 140.1)
106	131.5 (123.8, 159.3)	132.9 (124.2, 166.0)
106.5	138.4 (125.3, 300.4)	143.1 (126.5, 596.6)

TABLE 2

Point estimates (95% confidence intervals) for the upper limit to lifetime ι (in years) based on the profile likelihood ratio statistic $R(\iota)$ (middle) and the modified likelihood ratio statistic $R^*(\iota)$ for the tangent model approximation (right) using threshold exceedances of u for the Italian semi-super centenarian data set.

Figure 7 shows the profile likelihood and the modified version ℓ_{fr} for ι for two thresholds. The numbers of exceedances at these thresholds are appreciable, but nevertheless higher-order correction substantially increases the upper confidence limit for ι ; see also Table 2.

To assess the accuracy of the approximations, we can estimate the distribution of the likelihood root for ι using the bootstrap (cf. Lee & Young, 2005). We did not consider this approach in the simulation study, as its good properties have been checked in other contexts and its calibration entails a costly double parametric bootstrap. The b th bootstrap likelihood root $R^{(b)}(\iota)$ is computed at each value of ι based on a sample simulated from a generalized Pareto distribution with parameters $(\hat{\xi}_\iota, \iota)$. Figure 8 shows that the bootstrap p -value and the p -value obtained from the asymptotic χ_1^2 distribution of the profile likelihood ratio test agree up to Monte Carlo variability, and suggests that this approach may be useful more widely in the context of extremal inference.

The apparent stability of the estimates and the large standard errors for $\hat{\xi}_u$ seen in Table 1 do not allow us to rule out the exponential tail for thresholds $u > 107$ years, though the p -values for the four lowest thresholds 105–106.5 years, of 4.1%, 0.5%, 1.4% and 6.0%, are smaller. Under the exponential model, the probability of surviving one additional year conditional on survival up to u years is $\exp(-1/\sigma)$. Based on exceedances of $u = 110$ years, the model would yield an estimated probability of surviving an additional year of 0.476 with 95% confidence interval (0.416, 0.537): fewer than four in a thousand supercentenarians would be expected to live older than Emma Moreno.

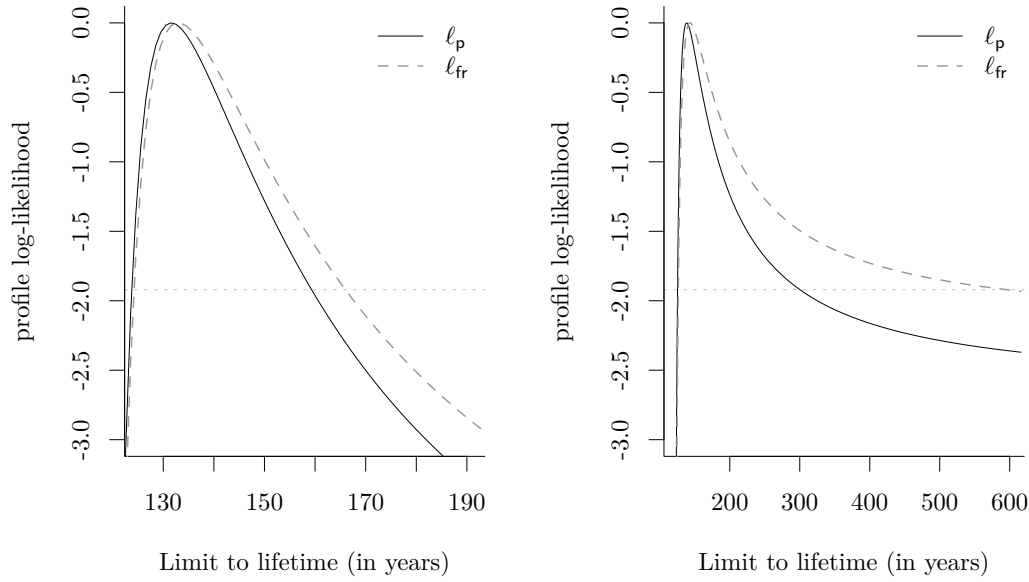


FIG 7. Profile likelihood ℓ_p (full black) and modified profile likelihood based on the tangent exponential model approximation ℓ_{fr} (dashed grey) as a function of the upper endpoint ι based on exceedances of lifetime beyond 106 years (left) and 106.5 years (right) for the Italian semi-supercenarian data. The horizontal dotted grey lines indicates cutoff values for the 95% confidence interval based on the asymptotic χ_1^2 distribution.

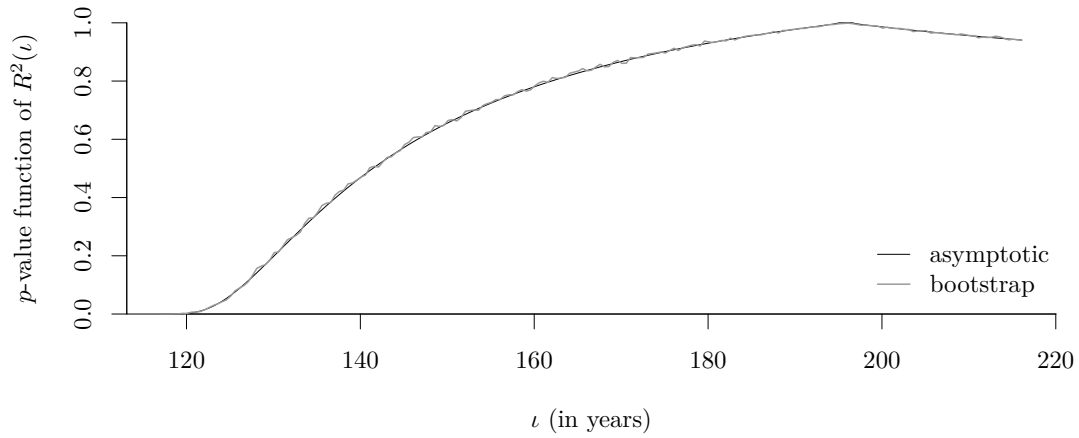


FIG 8. Italian semi-supercenarian data: p-value function for the profile likelihood ratio statistic $R^2(\iota) = 2\{\ell(\hat{\theta}) - \ell(\hat{\xi}_\iota)\}$ using excess lifetime above $u = 107$ years based on the asymptotic χ_1^2 distribution (black) and the bootstrap distribution $\#\{b : R^{2(b)}(\iota) > R^2(\iota)\}/B$ for bootstrap replications $b = 1, \dots, B$ (grey).

REFERENCES

- Barbi, E., Lagona, F., Marsili, M., Vaupel, J. W., & Wachter, K. W. (2018). The plateau of human mortality: Demography of longevity pioneers. *Science*, 360(6396), 1459–1461.
- Barndorff-Nielsen, O. E. & Cox, D. R. (1994). *Inference and Asymptotics*. London: Taylor & Francis.
- Belzile, L. R. (2019). *Contributions to Likelihood-Based Modelling of Extreme Values*. PhD thesis, EPFL, Lausanne.
- Brazzale, A. R., Davison, A. C., & Reid, N. (2007). *Applied Asymptotics: Case Studies in Small-Sample Statistics*. Cambridge: Cambridge University Press.
- Bücher, A. & Segers, J. (2017). On the maximum likelihood estimator for the generalized extreme-value distribution. *Extremes*, 20(4), 839–872.
- Coles, S. & Pericchi, L. (2003). Anticipating catastrophes through extreme value modelling. *Journal of the Royal Statistical Society, Series C (Applied Statistics)*, 52(4), 405–416.
- Coles, S., Pericchi, L. R., & Sisson, S. (2003). A fully probabilistic approach to extreme rainfall modeling. *Journal of Hydrology*, 273(1–4), 35–50.
- Cox, D. R., Isham, V. S., & Northrop, P. J. (2002). Floods: some probabilistic and statistical approaches. *Philosophical Transactions of the Royal Society of London A: Mathematical, Physical and Engineering Sciences*, 360(1796), 1389–1408.
- Cox, D. R. & Snell, E. J. (1968). A general definition of residuals (with Discussion). *Journal of the Royal Statistical Society, Series B (Methodological)*, 30(2), 248–275.
- Davison, A. C. (1986). Approximate predictive likelihood. *Biometrika*, 73, 323–332.
- Davison, A. C., Fraser, D. A. S., & Reid, N. (2006). Improved likelihood inference for discrete data. *Journal of the Royal Statistical Society, Series B (Statistical Methodology)*, 68, 495–508.
- Dombry, C. & Ferreira, A. (2019). Maximum likelihood estimators based on the block maxima method. *Bernoulli*, 25(3), 1690–1723.
- Einmahl, J. J., Einmahl, J. H. J., & de Haan, L. (2019). Limits to human life span through extreme value theory. *Journal of the American Statistical Association*, 114(527), 1075–1080.
- Embrechts, P., Klüppelberg, C., & Mikosch, T. (1997). *Modelling Extremal Events — For Insurance and Finance*. Berlin: Springer-Verlag.
- Fasiolo, M., Wood, S. N., Zaffran, M., Nedellec, R., & Goude, Y. (2020). Fast calibrated additive quantile regression. *Journal of the American Statistical Association*, to appear, 1–11.
- Firth, D. (1993). Bias reduction of maximum likelihood estimates. *Biometrika*, 80(1), 27–38.
- Fisher, R. A. & Tippett, L. H. C. (1928). Limiting forms of the frequency distribution of the largest or smallest member of a sample. *Mathematical Proceedings of the Cambridge Philosophical Society*, 24, 180–190.
- Fraser, D. A. S., Reid, N., & Wu, J. (1999). A simple general formula for tail probabilities for frequentist and Bayesian inference. *Biometrika*, 86(2), 249–264.
- Giles, D. E., Feng, H., & Godwin, R. T. (2016). Bias-corrected maximum likelihood estimation of the parameters of the generalized Pareto distribution. *Communications in Statistics - Theory and Methods*, 45(8), 2465–2483.
- Gnedenko, B. (1943). Sur la distribution limite du terme maximum d’une série aléatoire. *Annals of Mathematics. Second Series*, 44, 423–453.
- Grimshaw, S. D. (1993). Computing maximum likelihood estimates for the generalized Pareto distribution. *Technometrics*, 35(2), 185–191.
- Hanayama, N. & Sibuya, M. (2016). Estimating the upper limit of lifetime probability distribution, based on data of Japanese centenarians. *The Journals of Gerontology, Series A*, 71(8), 1014–1021.
- Hofert, M. & Mächler, M. (2016). Parallel and other simulations in R made easy: An end-to-end study. *Journal of Statistical Software*, 69(4), 1–44.
- Hosking, J. R. M. & Wallis, J. R. (1987). Parameter and quantile estimation for the generalized Pareto distribution. *Technometrics*, 29(3), 339–349.
- Kenne Pagui, E. C., Salvan, A., & Sartori, N. (2017). Median bias reduction of maximum likelihood estimates. *Biometrika*, 104, 923–928.
- Lee, S. M. & Young, G. A. (2005). Parametric bootstrapping with nuisance parameters. *Statistics & Probability Letters*, 71(2), 143–153.
- Papalexiou, S. M. & Koutsoyiannis, D. (2013). Battle of extreme value distributions: A global survey on extreme daily rainfall. *Water Resources Research*, 49(1), 187–201.

- Pickands, III, J. (1986). The continuous and differentiable domains of attraction of the extreme value distributions. *The Annals of Probability*, 14(3), 996–1004.
- Pirazzoli, P. A. (1982). Maree estreme a Venezia (periodo 1872–1981). *Acqua Aria*, 10, 1023–1039.
- Pires, J. F., Cysneiros, A. H. M. A., & Cribari-Neto, F. (2018). Improved inference for the generalized Pareto distribution. *Brazilian Journal of Probability and Statistics*, 32(1), 69–85.
- Roodman, D. (2018). Bias and size corrections in extreme value modeling. *Communications in Statistics - Theory and Methods*, 47(14), 3377–3391.
- Rootzén, H. & Zholud, D. (2017). Human life is unlimited — but short (with Discussion). *Extremes*, 20(4), 713–728.
- Severini, T. A. (1999). An empirical adjustment to the likelihood ratio statistic. *Biometrika*, 86(2), 235–247.
- Severini, T. A. (2000). *Likelihood Methods in Statistics*. New York: Oxford University Press.
- Skovgaard, I. M. (1996). An explicit large-deviation approximation to one-parameter tests. *Bernoulli*, 2(2), 145–165.
- Smith, R. L. (1985). Maximum likelihood estimation in a class of nonregular cases. *Biometrika*, 72(1), 67–90.
- Smith, R. L. (1986). Extreme value theory based on the r largest annual events. *Journal of Hydrology*, 86, 27–43.
- Smith, R. L. (1987). Approximations in extreme value theory. Technical Report 205, Center for Stochastic Processes, University of North Carolina Chapel Hill.

APPENDIX A: DETAILS OF THE SIMULATION STUDY

We used the infrastructure provided by the R package `simsalapar` (Hofert & Mächler, 2016) for the simulation study; the routines and higher-order methods described in the simulation study are implemented in the R package `mev` and the code used for the simulation study and the applications is available for download at <https://github.com/lbelzile/hoa-extremes>.

We obtained the maximum likelihood estimates for the generalized extreme value using an augmented Lagrange optimization routine with boundary constraints to ensure that $\hat{\xi} \geq -1$ and that $\hat{\sigma} + \hat{\xi}(x_i - \hat{\mu}) > 0$ ($i = 1, \dots, n$), so that the log likelihood was finite. The generalized Pareto distribution was fitted using the algorithm of Grimshaw (1993).

The profile log-likelihood estimates were obtained using constrained optimization methods at selected values of ψ , using dedicated algorithms such as sequential quadratic programming to obtain profile log-likelihood values for each of the values of ψ on a grid. The tangent space derivatives, canonical parameters, score and information matrices were derived analytically for every parameter and model of interest. The correction term Q for the tangent exponential model was calculated via eq. (3.4) and used to obtain $R^* = R + R^{-1} \log(Q/R)$. For the penalized likelihood of Severini, we computed penalty terms that were added to the profile log-likelihood values. Although the correction can be shown to be continuous, values of $R^*(\psi)$ can be numerically unstable when $\psi \approx \hat{\psi}$ (cf. Brazzale et al., 2007, p.149): the values of R^* can vary uncontrollably even though in principle $R^* \approx 0$ in a neighborhood of $\hat{\psi}$. The fact that $R^* \sim \text{No}(0, 1)$ suggests fitting constrained quantile regression B splines for the median of $R^* - R$ as a function of R , downweighting any observations near $R = 0$ with abnormal values. We then compare the predicted values for \hat{R}^* based on the spline fit with the calculated values, standardize the latter and exclude all points exceeding the $0.95 \chi_1^2$ quantile. A second spline regression is fitted to the remaining values in order to interpolate the missing values of R^* . This ad-hoc scheme usually affects estimates by less than $O(10^{-3})$, but is effective at removing the outliers and works well in practice. For the confidence intervals, we fitted constrained B -splines with response ψ and values R (respectively R^*) and predicted the quantile ψ corresponding to $2\ell_p(\psi) = \pm q$, where q is the $(1 - \alpha) \chi_1^2$ quantile. For the penalized methods, we computed the equivalent of the signed likelihood root statistic and proceeded analogously.

A.1. Parametric models. In addition to simulating data from a generalized extreme value distribution and from a generalized Pareto distribution with shape parameter $\xi \in \{-0.1, 0, 0.1\}$, we considered parametric families of distribution satisfying the extremal types theorem. These are

1. the standard normal distribution,
2. the standard log-normal distribution,
3. the Student- t distribution with 10 degrees of freedom,
4. the Burr distribution with survival function $S(x) = (1 + x^a)^{-b}$ with $a = 5, b = 2$,
5. the Weibull distribution with survival function $S(x) = \exp(-x^a)$ with $a = 2/3$,

Distribution	$q = 0.967$	$q = 0.978$	$q = 0.989$	$m = 30$	$m = 45$	$m = 90$	$m = 9000$	ξ^*
Burr	0.01	0.03	0.05	0.03	0.04	0.06	0.10	0.1
Weibull	0.15	0.13	0.11	0.16	0.14	0.12	0.05	0
Gen. gamma	0.15	0.14	0.12	0.17	0.15	0.13	0.07	0
Gaussian	-0.18	-0.16	-0.13	-0.16	-0.14	-0.12	-0.06	0
Lognormal	0.27	0.26	0.25	0.28	0.27	0.25	0.19	0
Student	-0.05	-0.03	0.00	-0.03	-0.02	0.01	0.07	0.1

TABLE 3

Penultimate shape parameters for six distributions, based on threshold exceedances above the q th quantile (columns 1–3), block maxima with maximum of m observations (columns 4–7). Even with blocks of size $m = 9000$, the penultimate shape can be far from the limiting tail index ξ^ reported in the last column.*

6. the generalized Gamma distribution with survival function

$$S(x) = \frac{\Gamma\left\{\frac{\gamma_1}{\gamma_2}, \left(\frac{x}{\beta}\right)^{\gamma_2}\right\}}{\Gamma\left(\frac{\gamma_1}{\gamma_2}\right)}, \quad x > 0, \gamma_1, \gamma_2, \beta > 0,$$

where $\Gamma(a, z) := \int_z^\infty x^{a-1} \exp(-x) dx$. The values for these parameters ($\beta = 1.83, \gamma_1 = 1.16$ and $\gamma_2 = 0.54$) were taken from Papalexiou & Koutsoyiannis (2013), so as to reflect values found by hydrologists in estimating the tail index for global rainfall.

Table 3 gives the limiting and penultimate shape parameters for various thresholds and block sizes. The Burr and Student distributions are heavy-tailed and have positive penultimate shape parameters, whereas the other distributions have different penultimate behaviours even though $\xi^* = 0$.

APPENDIX B: SIMULATION RESULTS

The discussed below tables may also be found in Appendix A of Belzile (2019). Tables 4 to 7 contain the estimated one-tailed error rates for the confidence intervals studied above, for data from a variety of underlying distributions, including the limiting generalized extreme-value and generalized Pareto distributions for maxima and threshold exceedances. Tables 8 to 11 contain the trimmed means of the relative bias of the point estimators for those same scenarios, whereas Tables 12 to 15 provide the estimated relative width of the confidence intervals relative to those of the profile likelihood method. We use trimmed means and discard the smallest and largest 10% of the simulations to remove confidence intervals that are extrapolated far beyond the range of the ψ values at which the profile likelihood is calculated, as these implausibly large intervals would be discarded by practitioners.

For the risk measures we consider, the point estimators provided by the TEM for the block maximum method are systematically larger than the maximum likelihood estimator, typically by 2%. They are positively biased when the (penultimate) shape is positive. The bias is more pronounced for the threshold method: maximum likelihood estimators are negatively biased and the TEM corrects for this in the case of correctly specified models F_7 – F_9 unless the sample size is too small ($k = 20$).

The TEM confidence intervals are at most 6% wider than profile likelihood intervals when $k = 60$ for the block maximum method, but up to 15% wider with $k = 20$ exceedances. The intervals provided by Severini’s modified profile likelihood based on the TEM approximation are narrower, and those based on empirical covariances are wider, than their profile likelihood

counterparts. For threshold exceedances with $k = 20$, the confidence intervals based on the modified likelihood root are sometimes twice as wide as those of the profile, whereas all the modified profile likelihoods have 30% longer intervals. The abysmal coverages for the Wald-based confidence intervals are due to the fact they are too short and to the asymmetry of the distributions of the corresponding estimators.

F	Parameter Method Error rate	Quantile						N -obs. mean					
		0.5	2.5	5	5	2.5	0.5	0.5	2.5	5	5	2.5	0.5
F_1	Wald	0.0	0.0	0.0	19.5	15.5	10.5	0.0	0.0	0.0	20.5	17.0	12.0
	profile	0.5	2.0	4.0	7.0	3.0	0.5	0.5	2.0	4.0	7.5	3.5	0.5
	TEM	0.5	2.5	5.0	5.0	2.0	0.5	0.5	2.5	4.5	5.5	2.5	0.5
	Severini (TEM)	0.5	1.5	3.5	8.0	3.5	0.5	0.5	1.5	3.5	8.5	4.0	0.5
	Severini (cov.)	0.5	2.0	4.5	5.0	2.0	0.5	0.5	2.5	4.5	5.5	2.0	0.5
F_2	Wald	0.0	0.0	1.5	13.0	10.5	7.0	0.0	0.0	1.0	13.0	10.5	7.0
	profile	0.5	2.5	5.0	4.5	2.5	0.5	0.5	3.0	6.0	4.0	2.0	0.5
	TEM	0.5	3.0	6.0	3.5	1.5	0.5	1.0	3.5	7.0	3.0	1.5	0.5
	Severini (TEM)	0.5	2.0	4.5	5.0	2.5	0.5	0.5	2.5	5.0	4.5	2.5	0.5
	Severini (cov.)	0.5	2.5	5.0	4.5	2.5	0.5	0.5	3.0	6.0	4.0	2.0	0.5
F_3	Wald	0.0	0.0	1.0	15.0	12.0	8.0	0.0	0.0	0.5	14.5	12.0	8.0
	profile	0.0	1.5	3.5	6.0	3.5	0.5	0.5	2.0	4.0	5.5	3.0	0.5
	TEM	0.0	1.5	4.0	5.0	2.5	0.5	0.5	2.0	5.0	4.5	2.0	0.5
	Severini (TEM)	0.0	1.0	3.0	6.5	3.5	1.0	0.0	1.5	3.5	6.0	3.0	0.5
	Severini (cov.)	0.0	1.5	3.0	6.0	3.0	0.5	0.5	2.0	4.0	5.5	3.0	0.5
F_4	Wald	0.0	0.0	0.0	26.0	22.5	17.0	0.0	0.0	0.0	27.5	24.0	18.0
	profile	0.5	1.5	3.5	10.0	5.5	1.0	0.5	1.5	3.0	10.5	5.5	1.0
	TEM	0.5	2.5	4.5	6.5	3.0	0.5	0.5	2.5	4.5	7.0	3.5	0.5
	Severini (TEM)	0.5	1.5	2.5	10.5	6.0	1.5	0.0	1.0	2.5	11.0	6.0	1.5
	Severini (cov.)	0.5	1.5	3.0	7.5	4.0	0.5	0.5	1.5	3.0	8.0	4.0	0.5
F_5	Wald	0.0	0.5	2.0	11.5	8.5	5.5	0.0	0.0	1.0	11.0	8.5	5.5
	profile	0.5	2.5	5.5	4.5	2.5	0.5	1.0	3.0	7.0	4.0	2.0	0.5
	TEM	0.5	2.5	5.5	3.5	2.0	0.5	1.0	3.5	7.0	3.5	1.5	0.5
	Severini (TEM)	0.5	2.0	4.5	5.0	2.5	0.5	0.5	2.5	5.5	4.5	2.5	0.5
	Severini (cov.)	0.5	2.5	5.0	4.5	2.5	0.5	0.5	3.0	6.5	4.0	2.0	0.5
F_6	Wald	0.0	0.0	0.5	22.5	19.0	13.5	0.0	0.0	0.0	24.5	20.5	15.0
	profile	0.5	2.0	4.0	10.0	5.5	1.5	0.5	2.0	3.5	11.0	6.0	1.5
	TEM	0.5	2.5	5.0	7.5	4.0	1.0	0.5	2.5	4.5	8.0	4.5	1.0
	Severini (TEM)	0.5	1.5	3.0	11.0	6.5	1.5	0.5	1.5	3.0	11.5	7.0	2.0
	Severini (cov.)	0.5	2.0	3.5	9.5	5.0	1.0	0.5	2.0	3.5	10.0	5.5	1.5
F_7	Wald	0.0	0.0	1.0	17.0	13.5	9.5	0.0	0.0	0.5	17.5	14.5	10.0
	profile	0.5	2.0	4.5	7.0	3.5	1.0	0.5	2.5	4.5	7.0	3.5	1.0
	TEM	0.5	2.5	5.5	5.5	2.5	0.5	0.5	3.0	5.5	5.5	3.0	0.5
	Severini (TEM)	0.5	2.0	4.0	8.0	4.0	1.0	0.5	2.0	4.0	8.0	4.5	1.0
	Severini (cov.)	0.5	2.0	4.0	7.0	3.5	1.0	0.5	2.5	4.5	7.0	3.5	1.0
F_8	Wald	0.0	0.0	0.5	19.0	15.5	11.0	0.0	0.0	0.5	19.5	16.5	12.0
	profile	0.5	2.0	4.5	7.0	3.5	1.0	0.5	2.0	4.5	7.0	3.5	1.0
	TEM	0.5	3.0	5.5	5.0	2.5	0.5	0.5	3.0	5.5	5.0	2.5	0.5
	Severini (TEM)	0.5	1.5	3.5	7.5	4.0	1.0	0.5	1.5	3.5	7.5	4.0	1.0
	Severini (cov.)	0.5	2.0	4.0	6.5	3.5	0.5	0.5	2.0	4.5	6.5	3.0	0.5
F_9	Wald	0.0	0.0	0.0	22.5	19.0	14.5	0.0	0.0	0.0	23.0	19.5	15.0
	profile	0.5	1.5	3.5	8.0	4.0	1.0	0.5	1.5	3.5	7.5	4.0	0.5
	TEM	0.5	2.5	5.0	5.0	2.5	0.5	0.5	2.5	5.0	5.0	2.0	0.0
	Severini (TEM)	0.0	1.0	2.5	8.5	4.5	1.0	0.0	1.0	2.5	8.0	4.0	0.5
	Severini (cov.)	0.0	1.5	3.0	6.5	3.0	0.5	0.5	1.5	3.5	6.5	3.0	0.5

TABLE 4

One-sided empirical error rates (%) for lower (first to third columns) and upper (fourth to sixth columns) confidence limits, block maximum method with $m = 45, k = 40$. The distributions (from top to bottom) are Burr (F_1), Weibull (F_2), generalized gamma (F_3), normal (F_4), lognormal (F_5), Student t (F_6), $\text{GEV}(\xi = 0.1)$ (F_7), Gumbel (F_8) and $\text{GEV}(\xi = -0.1)$ (F_9).

F	Parameter	Quantile						N -obs. mean					
		0.5	2.5	5	5	2.5	0.5	0.5	2.5	5	5	2.5	0.5
F_1	Wald	0.0	0.0	0.0	23.0	20.0	15.5	0.0	0.0	0.0	24.0	21.0	17.0
	profile	0.5	2.0	4.0	6.5	3.0	0.5	0.5	2.0	4.0	6.5	3.0	0.5
	TEM	0.5	2.5	5.0	3.5	1.5	0.0	0.5	2.5	5.0	3.5	1.5	0.0
	Severini (TEM)	0.0	1.0	3.0	7.5	3.5	0.5	0.0	1.0	3.0	7.5	3.5	0.5
	Severini (cov.)	0.5	2.0	4.5	3.0	1.0	0.0	0.5	3.0	6.0	3.0	1.0	0.0
F_2	Wald	0.0	0.0	0.5	20.0	17.5	13.5	0.0	0.0	0.0	20.0	17.5	13.5
	profile	0.5	2.0	4.0	6.0	3.0	0.5	0.5	2.5	4.5	5.5	2.5	0.5
	TEM	0.5	2.5	5.0	3.5	1.5	0.0	0.5	2.5	5.5	3.0	1.5	0.0
	Severini (TEM)	0.0	1.0	2.5	7.0	3.5	0.5	0.0	1.5	3.0	6.5	3.0	0.5
	Severini (cov.)	0.0	1.5	3.5	5.0	2.5	0.5	0.5	2.0	5.0	4.5	2.0	0.5
F_3	Wald	0.0	0.0	0.5	21.5	19.0	15.0	0.0	0.0	0.0	21.5	19.0	15.5
	profile	0.0	1.0	3.0	7.5	4.0	1.0	0.0	1.0	3.5	7.0	3.5	0.5
	TEM	0.0	1.5	3.5	5.0	2.5	0.0	0.5	1.5	4.0	4.5	2.0	0.0
	Severini (TEM)	0.0	0.5	1.5	9.0	5.0	1.0	0.0	0.5	2.0	8.5	4.5	1.0
	Severini (cov.)	0.0	1.0	2.5	6.5	3.5	0.5	0.0	1.5	3.5	6.0	3.0	0.5
F_4	Wald	0.0	0.0	0.0	28.5	25.5	20.5	0.0	0.0	0.0	29.0	26.0	21.5
	profile	0.5	1.5	3.5	7.0	3.5	0.5	0.5	1.5	3.5	6.5	3.0	0.5
	TEM	0.5	2.5	5.0	3.0	1.0	0.0	0.5	2.5	5.0	3.0	1.0	0.0
	Severini (TEM)	0.0	1.0	2.0	8.0	3.5	0.5	0.0	1.0	2.0	8.0	3.5	0.5
	Severini (cov.)	0.0	1.5	3.5	3.5	1.5	0.0	0.5	1.5	4.0	3.0	1.0	0.0
F_5	Wald	0.0	0.0	1.0	18.0	15.0	11.5	0.0	0.0	0.0	18.5	15.5	12.0
	profile	0.5	2.5	4.5	6.0	3.0	0.5	0.5	2.5	5.5	5.5	3.0	0.5
	TEM	0.5	2.5	5.0	4.5	2.0	0.5	1.0	3.0	6.0	4.0	2.0	0.5
	Severini (TEM)	0.0	1.5	3.0	7.0	4.0	1.0	0.5	1.5	4.0	7.0	3.5	1.0
	Severini (cov.)	0.5	2.0	4.0	5.5	3.0	0.5	0.5	3.0	6.0	5.0	2.5	0.5
F_6	Wald	0.0	0.0	0.0	25.5	22.0	17.5	0.0	0.0	0.0	27.0	23.5	19.0
	profile	0.5	2.0	4.0	8.5	4.5	1.0	0.5	2.0	4.0	8.0	4.0	1.0
	TEM	0.5	3.0	5.5	5.0	2.5	0.5	0.5	3.0	5.5	5.0	2.0	0.0
	Severini (TEM)	0.0	1.5	3.0	9.5	5.0	1.0	0.0	1.5	3.0	9.5	5.0	1.0
	Severini (cov.)	0.5	2.0	4.0	6.0	3.0	0.5	0.5	2.5	4.5	5.5	2.5	0.5
F_7	Wald	0.0	0.0	0.5	22.0	19.0	15.0	0.0	0.0	0.0	22.5	20.0	15.5
	profile	0.5	2.0	4.5	7.5	4.0	0.5	0.5	2.0	4.5	7.0	3.5	0.5
	TEM	0.5	2.5	5.5	5.0	2.0	0.5	0.5	2.5	5.5	4.5	2.0	0.5
	Severini (TEM)	0.0	1.5	3.0	8.5	4.5	1.0	0.0	1.5	3.0	8.5	4.5	1.0
	Severini (cov.)	0.5	1.5	4.0	6.5	3.0	0.5	0.5	2.5	5.0	6.0	3.0	0.5
F_8	Wald	0.0	0.0	0.0	23.5	20.5	16.5	0.0	0.0	0.0	24.0	21.0	17.0
	profile	0.5	2.0	4.0	7.0	3.5	0.5	0.5	2.0	4.0	6.5	3.0	0.5
	TEM	0.5	2.5	5.5	4.0	1.5	0.0	0.5	2.5	5.5	3.5	1.5	0.0
	Severini (TEM)	0.0	1.0	2.5	8.0	4.0	0.5	0.0	1.0	2.5	7.5	3.5	0.5
	Severini (cov.)	0.0	1.5	3.5	5.0	2.5	0.5	0.5	2.0	4.5	4.5	2.0	0.0
F_9	Wald	0.0	0.0	0.0	27.0	24.0	19.0	0.0	0.0	0.0	27.0	24.5	20.0
	profile	0.0	1.5	3.0	6.5	3.0	0.5	0.0	1.5	3.5	6.0	2.5	0.0
	TEM	0.5	2.5	5.0	2.5	1.0	0.0	0.5	2.5	5.0	2.5	0.5	0.0
	Severini (TEM)	0.0	0.5	1.5	7.5	3.5	0.5	0.0	0.5	2.0	6.5	3.0	0.0
	Severini (cov.)	0.0	1.0	3.0	4.0	1.5	0.0	0.0	1.5	3.5	3.0	1.0	0.0

TABLE 5

One-sided empirical error rates (%) for lower (first to third columns) and upper (fourth to sixth columns) confidence intervals, block maximum method with $m = 90$, $k = 20$. The distributions (from top to bottom) are Burr (F_1), Weibull (F_2), generalized gamma (F_3), normal (F_4), lognormal (F_5), Student t (F_6), GEV($\xi = 0.1$) (F_7), Gumbel (F_8) and GEV($\xi = -0.1$) (F_9).

F	Parameter Method Error rate	Quantile						N -obs. mean					
		0.5	2.5	5	5	2.5	0.5	0.5	2.5	5	5	2.5	0.5
F_1	Wald	0.0	0.0	0.0	29.0	26.0	20.5	0.0	0.0	0.0	31.5	28.5	23.5
	profile	0.5	1.5	3.0	5.5	1.5	0.0	0.5	1.5	3.5	5.0	1.0	0.0
	TEM	1.0	3.5	6.5	0.5	0.0	0.0	0.5	3.5	7.5	0.5	0.0	0.0
	Severini (TEM)	0.0	1.0	2.5	3.0	0.5	0.0	0.0	1.0	2.5	3.0	0.5	0.0
	Severini (cov.)	0.0	1.0	2.5	4.0	1.0	0.0	0.0	1.5	3.0	3.0	1.0	0.5
F_2	Wald	0.0	0.0	0.0	28.0	24.5	19.5	0.0	0.0	0.0	29.5	26.0	21.5
	profile	0.5	1.5	3.0	6.0	2.0	0.0	0.5	1.5	3.0	4.5	1.0	0.0
	TEM	0.5	3.0	6.0	0.5	0.0	0.0	0.5	3.5	7.0	0.0	0.0	0.0
	Severini (TEM)	0.0	1.0	2.0	3.0	1.0	0.0	0.0	1.0	2.5	2.5	0.5	0.0
	Severini (cov.)	0.0	1.0	2.0	3.5	1.0	0.0	0.0	1.0	3.0	2.5	1.0	0.5
F_3	Wald	0.0	0.0	0.0	28.0	25.5	21.0	0.0	0.0	0.0	29.5	26.5	22.5
	profile	0.0	0.5	2.0	7.0	2.5	0.0	0.0	1.0	2.5	5.5	2.0	0.0
	TEM	0.5	2.0	4.5	1.0	0.0	0.0	0.5	2.5	5.5	0.5	0.0	0.0
	Severini (TEM)	0.0	0.5	1.5	4.0	1.0	0.0	0.0	0.5	2.0	3.5	1.0	0.0
	Severini (cov.)	0.0	0.5	1.5	4.5	1.5	0.0	0.0	1.0	2.5	3.5	1.5	0.5
F_4	Wald	0.0	0.0	0.0	29.0	25.5	20.0	0.0	0.0	0.0	31.0	28.0	23.0
	profile	0.5	1.5	3.0	3.0	0.5	0.0	0.5	1.5	3.0	2.0	0.5	0.0
	TEM	1.0	3.5	7.0	0.0	0.0	0.0	1.0	3.5	6.5	0.0	0.0	0.0
	Severini (TEM)	0.0	1.0	2.0	1.5	0.0	0.0	0.0	1.0	2.0	1.0	0.0	0.0
	Severini (cov.)	0.0	0.5	2.0	2.5	1.0	0.0	0.0	1.0	2.0	2.0	1.0	0.5
F_5	Wald	0.0	0.0	0.0	28.5	25.0	20.5	0.0	0.0	0.0	29.5	26.5	22.0
	profile	0.0	1.5	3.0	8.0	3.5	0.0	0.5	2.0	4.0	7.0	3.0	0.0
	TEM	0.5	3.0	6.0	1.5	0.0	0.0	1.0	4.0	7.5	1.0	0.0	0.0
	Severini (TEM)	0.0	1.5	3.0	5.5	2.0	0.0	0.0	1.5	3.5	4.5	1.5	0.0
	Severini (cov.)	0.0	1.5	3.0	5.5	2.0	0.0	0.5	2.0	4.0	4.5	1.5	0.5
F_6	Wald	0.0	0.0	0.0	29.5	26.5	21.0	0.0	0.0	0.0	32.0	28.5	24.0
	profile	0.5	1.5	3.5	5.5	1.5	0.0	0.5	2.0	3.5	5.0	1.0	0.0
	TEM	1.0	4.0	7.5	0.5	0.0	0.0	1.0	4.0	7.5	0.5	0.0	0.0
	Severini (TEM)	0.0	1.5	3.0	3.0	0.5	0.0	0.0	1.0	3.0	3.0	0.5	0.0
	Severini (cov.)	0.0	1.0	2.5	4.0	1.5	0.0	0.5	1.5	3.0	3.5	1.5	0.5
F_7	Wald	0.0	0.0	0.0	29.0	25.5	20.5	0.0	0.0	0.0	30.5	27.5	22.5
	profile	0.5	1.5	3.0	6.0	2.0	0.0	0.5	1.5	3.5	5.5	1.5	0.0
	TEM	1.0	3.5	6.5	0.5	0.0	0.0	1.0	3.5	7.5	0.5	0.0	0.0
	Severini (TEM)	0.0	1.0	2.5	4.0	1.0	0.0	0.0	1.0	3.0	3.5	1.0	0.0
	Severini (cov.)	0.0	1.0	2.5	4.5	1.5	0.0	0.0	1.5	3.0	3.5	1.5	0.5
F_8	Wald	0.0	0.0	0.0	27.5	24.0	19.5	0.0	0.0	0.0	29.0	26.0	21.5
	profile	0.5	1.5	3.5	4.0	1.0	0.0	0.5	1.5	3.5	3.0	0.5	0.0
	TEM	0.5	3.5	6.5	0.0	0.0	0.0	0.5	3.5	7.0	0.0	0.0	0.0
	Severini (TEM)	0.0	1.0	2.0	2.0	0.5	0.0	0.0	1.0	2.5	2.0	0.5	0.0
	Severini (cov.)	0.0	0.5	2.0	3.0	1.0	0.0	0.0	1.0	3.0	2.5	1.0	0.5
F_9	Wald	0.0	0.0	0.0	28.0	24.0	18.5	0.0	0.0	0.0	29.5	26.5	21.0
	profile	0.5	1.0	2.5	2.5	0.5	0.0	0.5	1.5	2.5	1.5	0.0	0.0
	TEM	1.0	3.5	6.5	0.0	0.0	0.0	0.5	3.0	6.5	0.0	0.0	0.0
	Severini (TEM)	0.0	0.5	1.5	1.0	0.0	0.0	0.0	0.5	1.0	0.5	0.0	0.0
	Severini (cov.)	0.0	0.5	1.5	2.0	0.5	0.0	0.0	1.0	2.0	1.5	1.0	0.5

TABLE 6

One-sided empirical error rates (%) for lower (first to third columns) and upper (fourth to sixth columns) confidence limits, peaks-over-threshold method with $k = 20$. The distributions (from top to bottom) are Burr (F_1), Weibull (F_2), generalized gamma (F_3), normal (F_4), lognormal (F_5), Student t (F_6), GP($\xi = 0.1$) (F_7), exponential (F_8) and GP($\xi = -0.1$) (F_9).

F	Parameter Method Error rate	Quantile						N -obs. mean					
		0.5	2.5	5	5	2.5	0.5	0.5	2.5	5	5	2.5	0.5
F_1	Wald	0.0	0.0	0.0	24.0	20.0	14.5	0.0	0.0	0.0	25.5	22.0	16.5
	profile	0.5	1.5	3.5	9.5	4.5	0.5	0.5	1.5	3.0	10.0	4.5	0.5
	TEM	0.5	3.0	5.5	4.5	1.5	0.0	0.5	2.5	5.5	5.0	2.0	0.0
	Severini (TEM)	0.5	1.5	3.5	8.0	3.5	0.5	0.5	1.5	3.5	8.5	4.0	0.5
	Severini (cov.)	0.5	1.5	3.5	8.0	3.5	0.5	0.5	1.5	3.5	8.5	4.0	0.5
F_2	Wald	0.0	0.0	0.0	19.5	16.5	11.5	0.0	0.0	0.0	19.5	16.5	12.0
	profile	0.5	1.5	3.5	7.5	4.0	1.0	0.5	2.0	3.5	7.5	4.0	1.0
	TEM	0.5	3.0	5.5	4.0	2.0	0.5	0.5	3.0	6.0	4.0	1.5	0.5
	Severini (TEM)	0.5	2.0	3.5	6.5	3.5	0.5	0.5	2.0	4.0	6.0	3.0	0.5
	Severini (cov.)	0.5	2.0	3.5	6.5	3.5	0.5	0.5	2.0	4.0	6.0	3.0	0.5
F_3	Wald	0.0	0.0	0.0	21.0	18.0	13.0	0.0	0.0	0.0	21.0	18.0	13.5
	profile	0.0	1.0	2.0	9.0	5.5	1.5	0.0	1.0	2.5	9.0	5.0	1.0
	TEM	0.0	2.0	4.0	5.0	2.5	0.5	0.5	2.0	5.0	5.0	2.5	0.5
	Severini (TEM)	0.0	1.0	2.5	8.0	4.5	1.0	0.0	1.0	3.0	8.0	4.5	1.0
	Severini (cov.)	0.0	1.0	2.5	8.0	4.5	1.0	0.0	1.5	3.0	8.0	4.5	1.0
F_4	Wald	0.0	0.0	0.0	30.0	26.5	20.5	0.0	0.0	0.0	32.0	28.0	22.5
	profile	0.5	1.5	3.0	11.0	6.0	1.0	0.5	1.0	2.5	11.5	6.0	1.0
	TEM	0.5	3.0	5.0	4.5	2.0	0.0	0.5	2.5	4.5	5.0	2.0	0.0
	Severini (TEM)	0.0	1.0	2.5	9.5	4.5	0.5	0.0	1.0	2.0	9.5	5.0	0.5
	Severini (cov.)	0.0	1.0	2.5	9.0	4.5	0.5	0.0	1.0	2.5	9.5	4.5	0.5
F_5	Wald	0.0	0.0	0.5	17.0	14.0	9.5	0.0	0.0	0.0	17.5	14.5	10.0
	profile	0.5	2.0	3.5	7.5	4.0	1.0	0.5	2.0	4.0	7.0	4.0	1.0
	TEM	0.5	3.0	5.5	4.5	2.0	0.5	1.0	3.5	7.0	4.5	2.0	0.5
	Severini (TEM)	0.5	2.0	4.0	6.5	3.5	1.0	0.5	2.5	5.0	6.5	3.5	0.5
	Severini (cov.)	0.5	2.0	4.0	6.5	3.5	1.0	0.5	2.5	5.0	6.5	3.5	0.5
F_6	Wald	0.0	0.0	0.0	27.0	23.5	18.0	0.0	0.0	0.0	29.0	25.0	19.5
	profile	0.5	2.0	3.5	12.5	7.0	2.0	0.5	1.5	3.0	13.5	7.5	2.0
	TEM	0.5	3.0	5.5	7.0	3.5	0.5	0.5	2.5	5.5	7.5	4.0	0.5
	Severini (TEM)	0.5	1.5	3.5	11.0	6.5	1.5	0.5	1.5	3.5	11.5	6.5	1.5
	Severini (cov.)	0.5	1.5	3.5	11.0	6.5	1.5	0.5	1.5	3.5	11.5	6.5	1.5
F_7	Wald	0.0	0.0	0.0	21.5	18.0	13.0	0.0	0.0	0.0	22.5	19.0	14.0
	profile	0.5	1.5	3.5	9.5	5.5	1.5	0.5	1.5	3.5	10.0	5.5	1.5
	TEM	0.5	3.0	5.5	5.5	3.0	0.5	0.5	3.0	6.0	5.5	3.0	0.5
	Severini (TEM)	0.5	2.0	4.0	8.5	5.0	1.0	0.5	2.0	4.0	8.5	5.0	1.0
	Severini (cov.)	0.5	2.0	4.0	8.5	5.0	1.0	0.5	2.0	4.0	8.5	4.5	1.0
F_8	Wald	0.0	0.0	0.0	23.0	19.5	14.5	0.0	0.0	0.0	23.5	20.5	15.5
	profile	0.5	1.5	3.5	9.0	5.0	1.0	0.5	1.5	3.5	9.0	5.0	1.0
	TEM	0.5	3.0	5.5	4.5	2.0	0.5	0.5	3.0	5.5	4.5	2.0	0.5
	Severini (TEM)	0.0	1.5	3.5	7.5	4.0	1.0	0.0	1.5	3.5	7.5	4.0	1.0
	Severini (cov.)	0.5	1.5	3.5	7.5	4.0	1.0	0.0	1.5	3.5	7.5	4.0	0.5
F_9	Wald	0.0	0.0	0.0	27.5	23.5	18.0	0.0	0.0	0.0	28.0	24.5	19.0
	profile	0.5	1.5	2.5	9.5	5.0	0.5	0.5	1.0	2.5	9.5	5.0	0.5
	TEM	0.5	2.5	5.0	4.0	1.5	0.0	0.5	2.5	5.0	3.5	1.5	0.0
	Severini (TEM)	0.0	1.0	2.5	8.0	4.0	0.5	0.0	1.0	2.5	8.0	3.5	0.5
	Severini (cov.)	0.0	1.0	2.5	8.0	3.5	0.5	0.0	1.0	2.5	8.0	3.5	0.5

TABLE 7

One-sided empirical error rates (%) for lower (first to third columns) and upper (fourth to sixth columns) confidence limits, peaks-over-threshold method with $k = 60$. The distributions (from top to bottom) are Burr (F_1), Weibull (F_2), generalized gamma (F_3), normal (F_4), lognormal (F_5), Student t (F_6), GP($\xi = 0.1$) (F_7), exponential (F_8) and GP($\xi = -0.1$) (F_9).

Parameter	Method F	F_1	F_2	F_3	F_4	F_5	F_6	F_7	F_8	F_9
Quantile	MLE	-1	5	2	-3	9	-3	1	0	-2
	TEM	1	7	5	-1	10	-1	3	2	0
	Severini (TEM)	-2	3	0	-3	4	-4	-1	-1	-2
	Severini (cov.)	0	5	2	-2	7	-3	0	0	-1
N -obs. median	MLE	-1	7	4	-3	11	-4	1	0	-2
	TEM	1	9	7	-1	13	-1	3	2	1
	Severini (TEM)	-2	4	1	-4	6	-5	-1	-1	-2
	Severini (cov.)	1	6	3	-2	9	-3	1	0	-1
N -obs. mean	MLE	-1	10	7	-3	19	-4	2	0	-2
	TEM	1	13	10	-1	20	-1	5	3	1
	Severini (TEM)	-2	6	3	-4	12	-5	0	-1	-2
	Severini (cov.)	1	10	6	-2	17	-4	2	1	-1

TABLE 8

Truncated mean ($\alpha = 0.1$) of relative bias (in %), block maximum method with $m = 45, k = 40$. The largest standard error, obtained using a nonparametric bootstrap, is 0.51%. The distributions (from top to bottom) are Burr (F_1), Weibull (F_2), generalized gamma (F_3), normal (F_4), lognormal (F_5), Student t (F_6), GEV($\xi = 0.1$) (F_7), Gumbel (F_8) and GEV($\xi = -0.1$) (F_9).

Parameter	Method F	F_1	F_2	F_3	F_4	F_5	F_6	F_7	F_8	F_9
Quantile	MLE	0	3	1	-2	7	-2	1	0	-2
	TEM	2	6	5	1	10	2	4	3	1
	Severini (TEM)	-2	-1	-3	-3	0	-4	-3	-2	-3
	Severini (cov.)	3	4	2	0	8	1	2	2	0
N -obs. median	MLE	1	4	2	-2	10	-1	2	0	-2
	TEM	3	8	6	1	13	2	5	4	2
	Severini (TEM)	-2	-1	-2	-3	1	-4	-3	-2	-3
	Severini (cov.)	4	6	4	0	11	1	4	3	1
N -obs. mean	MLE	2	9	6	-2	21	-1	5	2	-1
	TEM	5	13	10	1	23	3	8	6	2
	Severini (TEM)	-1	2	0	-3	7	-4	-1	-1	-3
	Severini (cov.)	9	12	9	1	25	3	8	5	2

TABLE 9

Truncated mean ($\alpha = 0.1$) of relative bias (in %), block maximum method with $m = 90, k = 20$. The largest standard error, obtained using a nonparametric bootstrap, is 0.81%. The distributions (from top to bottom) are Burr (F_1), Weibull (F_2), generalized gamma (F_3), normal (F_4), lognormal (F_5), Student t (F_6), GEV($\xi = 0.1$) (F_7), Gumbel (F_8) and GEV($\xi = -0.1$) (F_9).

Parameter	Method F	F_1	F_2	F_3	F_4	F_5	F_6	F_7	F_8	F_9
Quantile	MLE	-3	-4	-5	-2	-6	-4	-4	-3	-2
	TEM	2	3	2	1	3	2	3	3	1
	Severini (TEM)	-1	-1	-2	-1	-2	-1	-1	0	-1
	Severini (cov.)	-1	-1	-2	-1	-2	-1	-1	-1	-1
N -obs. median	MLE	-3	-4	-5	-3	-6	-4	-5	-3	-2
	TEM	2	4	3	1	5	2	3	3	2
	Severini (TEM)	0	0	-1	-1	-1	-1	-1	0	0
	Severini (cov.)	0	0	-1	-1	0	-1	0	0	0
N -obs. mean	MLE	-3	-3	-4	-3	-3	-4	-4	-2	-2
	TEM	4	8	7	2	14	4	7	5	3
	Severini (TEM)	1	3	2	-1	6	0	2	1	0
	Severini (cov.)	1	4	3	0	8	1	3	2	0

TABLE 10

Truncated mean ($\alpha = 0.1$) of relative bias (in %), peaks-over-threshold method with $k = 20$. The largest standard error, obtained using a nonparametric bootstrap, is 0.77%. The distributions (from top to bottom) are Burr (F_1), Weibull (F_2), generalized gamma (F_3), normal (F_4), lognormal (F_5), Student t (F_6), GP($\xi = 0.1$) (F_7), exponential (F_8) and GP($\xi = -0.1$) (F_9).

Parameter	Method F	F_1	F_2	F_3	F_4	F_5	F_6	F_7	F_8	F_9
Quantile	MLE	-3	-2	-4	-4	-1	-5	-3	-3	-3
	TEM	-1	2	0	-2	4	-3	0	0	-1
	Severini (TEM)	-2	0	-2	-3	2	-4	-2	-2	-2
	Severini (cov.)	-2	0	-2	-3	2	-4	-2	-2	-2
N -obs. median	MLE	-3	-1	-4	-4	0	-6	-4	-3	-3
	TEM	-1	3	0	-2	5	-3	0	0	-1
	Severini (TEM)	-2	1	-2	-4	3	-5	-2	-2	-3
	Severini (cov.)	-2	1	-2	-4	3	-5	-2	-2	-3
N -obs. mean	MLE	-4	0	-3	-5	4	-7	-3	-3	-3
	TEM	-1	5	2	-3	11	-4	1	0	-1
	Severini (TEM)	-2	3	0	-4	8	-5	-1	-1	-3
	Severini (cov.)	-2	3	0	-4	8	-5	-1	-1	-2

TABLE 11

Truncated mean ($\alpha = 0.1$) of relative bias (in %), peaks-over-threshold method with $k = 60$. The largest standard error, obtained using a nonparametric bootstrap, is 0.49%. The distributions (from top to bottom) are Burr (F_1), Weibull (F_2), generalized gamma (F_3), normal (F_4), lognormal (F_5), Student t (F_6), GP($\xi = 0.1$) (F_7), exponential (F_8) and GP($\xi = -0.1$) (F_9).

F	Parameter Method Conf. level (%)	Quantile			N -obs. median			N -obs. mean		
		90	95	99	90	95	99	90	95	99
F_1	Wald	68	59	44	67	58	42	61	52	35
	TEM	103	103	103	104	103	103	104	104	104
	Severini (TEM)	93	93	92	93	93	92	92	91	91
	Severini (cov.)	105	105	105	106	106	105	111	111	112
F_2	Wald	66	58	45	65	58	44	60	52	39
	TEM	102	102	102	102	102	102	102	102	102
	Severini (TEM)	92	92	92	92	92	92	91	91	91
	Severini (cov.)	97	96	96	97	97	96	97	97	97
F_3	Wald	66	58	44	65	57	44	59	51	37
	TEM	102	102	102	102	102	102	102	102	102
	Severini (TEM)	92	92	92	92	92	92	91	91	91
	Severini (cov.)	96	96	96	96	96	96	96	96	96
F_4	Wald	64	58	47	64	58	46	62	55	43
	TEM	108	108	107	108	108	107	108	108	108
	Severini (TEM)	97	96	96	96	96	96	96	96	96
	Severini (cov.)	104	104	104	104	104	103	105	105	104
F_5	Wald	67	58	42	66	57	40	55	44	28
	TEM	99	99	98	99	99	99	98	98	97
	Severini (TEM)	90	89	88	89	89	88	86	85	85
	Severini (cov.)	94	94	93	94	94	94	93	93	93
F_6	Wald	68	60	46	67	59	44	63	54	38
	TEM	104	104	104	105	105	105	105	105	105
	Severini (TEM)	94	94	93	94	94	93	93	93	92
	Severini (cov.)	100	99	99	100	99	99	100	100	99
F_7	Wald	67	59	44	66	58	43	60	51	35
	TEM	102	102	102	103	102	102	103	103	102
	Severini (TEM)	92	92	91	92	92	91	91	90	90
	Severini (cov.)	97	96	96	96	96	96	96	96	95
F_8	Wald	66	59	46	65	58	46	62	54	42
	TEM	105	105	104	105	105	105	105	105	105
	Severini (TEM)	94	94	94	94	94	94	93	93	94
	Severini (cov.)	99	99	98	99	99	98	99	99	99
F_9	Wald	64	59	49	64	59	49	62	57	46
	TEM	107	107	106	107	107	106	108	107	106
	Severini (TEM)	96	96	96	96	96	96	96	96	95
	Severini (cov.)	102	102	101	102	102	101	102	102	101

TABLE 12

Truncated mean ($\alpha = 0.1$) of the ratio of the confidence interval width relative to the width of profile confidence interval (in %), block maximum method with $m = 45, k = 40$. The largest standard error, obtained using a nonparametric bootstrap, is 0.13%. The distributions (from top to bottom) are Burr (F_1), Weibull (F_2), generalized gamma (F_3), normal (F_4), lognormal (F_5), Student t (F_6), GEV($\xi = 0.1$) (F_7), Gumbel (F_8) and GEV($\xi = -0.1$) (F_9).

F	Parameter Method Conf. level (%)	Quantile			N -obs. median			N -obs. mean		
		90	95	99	90	95	99	90	95	99
F_1	Wald	46	37	22	45	36	22	37	28	15
	TEM	105	105	105	106	106	106	106	106	106
	Severini (TEM)	85	84	83	85	84	83	81	80	81
	Severini (cov.)	117	118	118	118	118	117	149	151	149
F_2	Wald	47	39	26	47	38	26	40	32	22
	TEM	104	105	104	105	105	104	105	105	104
	Severini (TEM)	85	85	85	85	85	86	82	83	85
	Severini (cov.)	102	101	100	102	102	101	103	102	101
F_3	Wald	47	39	25	46	38	25	39	31	20
	TEM	104	105	104	105	105	104	104	104	104
	Severini (TEM)	85	85	85	85	85	85	82	82	84
	Severini (cov.)	101	100	99	101	101	100	101	101	100
F_4	Wald	47	40	29	47	40	29	43	36	25
	TEM	114	114	112	115	114	111	115	114	111
	Severini (TEM)	92	92	91	92	91	91	90	89	89
	Severini (cov.)	116	116	113	116	115	112	122	121	118
F_5	Wald	46	36	21	44	34	20	31	22	12
	TEM	98	98	98	98	98	98	96	96	96
	Severini (TEM)	80	78	77	79	78	78	72	72	75
	Severini (cov.)	98	97	97	98	98	98	101	100	101
F_6	Wald	47	38	24	46	37	23	39	30	17
	TEM	107	107	107	108	108	108	108	108	108
	Severini (TEM)	87	86	84	86	85	85	83	82	83
	Severini (cov.)	108	107	107	107	107	106	113	113	112
F_7	Wald	47	37	23	45	36	22	37	28	16
	TEM	104	104	104	104	104	104	104	104	104
	Severini (TEM)	84	83	82	84	83	83	80	79	80
	Severini (cov.)	101	101	100	101	101	100	103	102	101
F_8	Wald	48	40	28	47	39	28	42	35	24
	TEM	109	109	108	109	109	108	110	109	107
	Severini (TEM)	89	88	88	88	88	88	86	86	87
	Severini (cov.)	106	105	104	106	105	103	108	107	105
F_9	Wald	49	42	32	48	42	32	45	39	30
	TEM	114	113	110	114	112	109	114	112	108
	Severini (TEM)	92	92	91	92	91	91	90	90	89
	Severini (cov.)	112	110	108	111	109	107	113	112	108

TABLE 13

Truncated mean ($\alpha = 0.1$) of the ratio of the confidence interval width relative to the width of profile confidence interval (in %), block maximum method with $m = 90, k = 20$. The largest standard error, obtained using a nonparametric bootstrap, is 0.34%. The distributions (from top to bottom) are Burr (F_1), Weibull (F_2), generalized gamma (F_3), normal (F_4), lognormal (F_5), Student t (F_6), GEV($\xi = 0.1$) (F_7), Gumbel (F_8) and GEV($\xi = -0.1$) (F_9).

F	Parameter Method Conf. level (%)	Quantile			N -obs. median			N -obs. mean		
		90	95	99	90	95	99	90	95	99
F_1	Wald	34	24	11	32	22	11	22	14	6
	TEM	203	202	179	207	202	172	253	238	184
	Severini (TEM)	127	127	127	128	128	127	135	133	126
	Severini (cov.)	131	131	131	133	133	131	142	140	130
F_2	Wald	36	26	14	35	25	14	26	18	10
	TEM	192	186	158	193	184	152	221	205	168
	Severini (TEM)	126	126	125	126	126	124	129	127	121
	Severini (cov.)	130	130	128	131	131	128	135	133	125
F_3	Wald	36	26	14	34	25	14	24	17	9
	TEM	193	189	162	195	187	155	224	206	168
	Severini (TEM)	126	126	125	126	126	124	130	128	123
	Severini (cov.)	131	131	129	132	132	129	137	134	126
F_4	Wald	37	29	18	36	28	18	30	22	14
	TEM	182	171	144	182	168	140	201	187	157
	Severini (TEM)	124	123	120	124	122	118	122	119	112
	Severini (cov.)	128	126	121	129	127	121	128	125	116
F_5	Wald	34	23	10	32	21	9	18	10	4
	TEM	211	213	189	217	214	179	293	266	184
	Severini (TEM)	130	130	129	131	131	128	144	141	129
	Severini (cov.)	134	135	132	136	136	132	152	148	132
F_6	Wald	35	25	12	33	23	11	24	15	7
	TEM	203	202	179	207	202	172	248	235	185
	Severini (TEM)	126	127	127	127	128	127	133	132	126
	Severini (cov.)	130	131	130	132	133	131	140	138	129
F_7	Wald	35	24	12	33	23	11	22	14	6
	TEM	203	201	176	207	201	168	252	235	180
	Severini (TEM)	127	127	127	128	128	127	135	133	126
	Severini (cov.)	131	132	131	133	133	131	142	140	129
F_8	Wald	37	28	16	35	27	16	28	20	12
	TEM	186	178	151	187	175	146	209	195	162
	Severini (TEM)	124	124	122	125	124	121	125	122	115
	Severini (cov.)	129	129	125	130	129	125	131	129	120
F_9	Wald	39	31	21	37	30	21	33	26	18
	TEM	170	158	136	168	155	133	185	171	148
	Severini (TEM)	122	121	117	122	120	115	120	116	110
	Severini (cov.)	126	123	117	126	123	117	125	120	112

TABLE 14

Truncated mean ($\alpha = 0.1$) of the ratio of the confidence interval width relative to the width of profile confidence interval (in %), peaks-over-threshold method with $k = 20$. The largest standard error, obtained using a nonparametric bootstrap, is 1.17%. The distributions (from top to bottom) are Burr (F_1), Weibull (F_2), generalized gamma (F_3), normal (F_4), lognormal (F_5), Student t (F_6), GP($\xi = 0.1$) (F_7), exponential (F_8) and GP($\xi = -0.1$) (F_9).

F	Parameter Method Conf. level (%)	Quantile			N -obs. median			N -obs. mean		
		90	95	99	90	95	99	90	95	99
F_1	Wald	64	53	36	62	52	34	55	44	26
	TEM	127	128	130	130	131	131	137	138	138
	Severini (TEM)	108	108	108	109	109	109	111	111	111
	Severini (cov.)	108	108	108	109	109	109	111	111	111
F_2	Wald	62	53	38	61	52	37	55	45	30
	TEM	126	127	127	128	128	128	133	133	131
	Severini (TEM)	108	108	108	108	108	108	110	110	109
	Severini (cov.)	108	108	108	108	109	109	110	110	110
F_3	Wald	62	53	37	61	52	36	55	44	29
	TEM	126	127	128	128	129	129	134	135	132
	Severini (TEM)	108	108	108	108	108	109	110	110	110
	Severini (cov.)	108	108	109	108	109	109	110	111	110
F_4	Wald	60	53	40	59	52	39	57	49	36
	TEM	126	127	126	128	128	127	131	131	129
	Severini (TEM)	108	108	107	108	108	107	109	109	108
	Severini (cov.)	108	108	108	108	108	108	109	109	108
F_5	Wald	64	53	34	63	51	32	50	37	20
	TEM	127	129	132	130	132	133	144	146	143
	Severini (TEM)	108	109	109	109	110	110	113	114	114
	Severini (cov.)	109	109	110	110	110	110	114	114	114
F_6	Wald	64	54	37	63	53	36	57	46	29
	TEM	127	128	130	130	131	131	137	137	137
	Severini (TEM)	108	108	108	109	109	109	111	110	110
	Severini (cov.)	108	108	108	109	109	109	111	111	111
F_7	Wald	63	53	36	62	52	35	55	43	26
	TEM	128	128	130	130	131	131	138	138	137
	Severini (TEM)	108	108	108	109	109	109	111	111	111
	Severini (cov.)	108	108	109	109	109	109	111	111	111
F_8	Wald	62	54	39	61	53	38	57	48	34
	TEM	126	126	126	127	128	127	131	131	129
	Severini (TEM)	107	108	108	108	108	108	109	109	109
	Severini (cov.)	108	108	108	108	108	108	109	109	109
F_9	Wald	60	54	42	60	53	42	58	51	39
	TEM	125	125	123	126	126	123	128	127	124
	Severini (TEM)	108	107	107	108	107	106	108	108	106
	Severini (cov.)	108	108	107	108	108	107	109	108	107

TABLE 15

Truncated mean ($\alpha = 0.1$) of the ratio of the confidence interval width relative to the width of profile confidence interval (in %), peaks-over-threshold method with $k = 60$. The largest standard error, obtained using a nonparametric bootstrap, is 0.12%. The distributions (from top to bottom) are Burr (F_1), Weibull (F_2), generalized gamma (F_3), normal (F_4), lognormal (F_5), Student t (F_6), GP($\xi = 0.1$) (F_7), exponential (F_8) and GP($\xi = -0.1$) (F_9).